I. STUDY OF THE EFFECT OF INTEGRATION STEP SIZE IN QUASICLASSICAL TRAJECTORY CALCULATIONS

II. STUDY OF THE ROLE OF VIBRATIONAL ENERGY IN REACTIVE COLLISIONS: $He + H_2^+ \rightarrow HeH^+ + H$ USING SPLINEFITTED AB INITIO AND DIM POTENTIAL-ENERGY SURFACES

By

RADHA RANGARAJAN

Bachelor of Science

Annamalai University

Annamalainagar, India

1974

Submitted to the Faculty of the Graduate College
of the Oklahoma State University
in partial fulfillment of the requirements
for the Degree of
MASTER OF SCIENCE
December, 1975

Thesis
1975
R 196s
Cop. 2

OKLAHOMA
STATE UNIVERSITY
LIBRARY

MAR 24 1976

I. STUDY OF THE EFFECT OF INTEGRATION STEP SIZE IN QUASICLASSICAL TRAJECTORY CALCULATIONS

II. STUDY OF THE ROLE OF VIBRATIONAL ENERGY IN REACTIVE COLLISIONS: $He + H_2^+ \rightarrow HeH^+ + H$ USING SPLINEFITTED AB INITIO AND DIM POTENTIAL-ENERGY SURFACES

Thesis Approved:

Lionel M. Raff
Thesis Adviser

J. Paul Devlin

N. N. Durham
Dean of the Graduate College

935672

To my Parents

ACKNOWLEDGEMENTS

It is with great pleasure that I express my sincere gratitude and appreciation to Dr. Lionel M. Raff who suggested and supervised this research work. His guidance and encouragement have been invaluable to me throughout my career.

The constant and loving encouragements given by my mother, Rajalakshmi, my father, Dr. T. Rangarajan, my sisters, Geetha, Revathi, and Vimal and by my brother Ravi are gratefully acknowledged.

I am highly thankful to Dr. N. Sathyamurthy for his assistance and helpful suggestions and for teaching me many things during the course of this investigation.

I gratefully acknowledge Dr. Gilbert J. Mains and Dr. J. Paul Devlin for serving as members of my advisory committee.

I sincerely thank Mr. G. Prakash who critically proof-read the manuscript for both the contents and get-up.

Financial support by the Department of Chemistry through a teaching assistantship, a special summer scholarship and NSF Grant NPS71-03499-A02 through a research assistantship are gratefully acknowledged.

I gratefully acknowledge the Graduate College of OSU and the Department of Chemistry for the Graduate Excellence Award.

Finally, I thank Mrs. Peggy Peaden for her superb job in typing the final copy of the thesis.

TABLE OF CONTENTS

LIST OF TABLES

LIST OF FIGURES

LIST OF FIGURES (Continued)

PART I

STUDY OF THE EFFECT OF INTEGRATION STEP SIZE IN QUASICLASSICAL TRAJECTORY CALCULATIONS

CHAPTER I

INTRODUCTION

The method of quasiclassical trajectories (1) has been of immense use in the investigation of reaction dynamics. It has been successfully employed in studying molecular beam kinetics of the deuterium atom-hydrogen halide exchange reactions (2), predicting the mechanism of hydrogen-iodine reactions (3), computing energy distributions in chemical laser reactions (4) and calculating the rates of methane + hot tritium atom reactions (5). For a long list of other quasiclassical trajectory studies, the reader is referred to the recent reviews (6). Despite its success in the field of molecular dynamics, the method has a serious disadvantage in that it needs large computing facilities. This is so because numerous trajectories must be computed to simulate the experimental conditions. Each trajectory is computed by integrating Hamilton's equations (7) numerically by a Runge-Kutta-Gill or related procedures (8) for a given set of initial conditions. The integration stepsize is usually selected by checking for the conservation of energy and total angular momenta at the beginning and at the end of each trajectory. Back-integration and stepsize reductions are also used to test the accuracy of the integration method.

Several studies (9) have employed various stepsizes ranging from 0.002 to 0.5 molecular units (3), as shown in Table I. It should be noted that in the large majority of cases the stepsize was less than

TABLE I

SUMMARY OF STEPSIZES USED IN DIFFERENT QUASICLASSICAL TRAJECTORY STUDIES

Reference	System Studied	Integration Method	Stepsize (DT)*
1a	$H + H_2$	Runge-Kutta-Gill	0.046
2	D + ClH	Runge-Kutta-Gill	0.02
9a	H + HF	Runge-Kutta-Gill	0.0373
9b	$H + X_2$ X + HY	Runge-Kutta-Gill	0.0557
9c	$H + H_2$	Runge-Kutta-Gill	0.0373
9d	Cl + HI Cl + DI	Fourth order Adams-Moulton	0.0557
9e	A + BC	Runge-Kutta-Gill	0.0557; 0.111
9f	A + BC	Higher order Adams-Moulton	0.0557; 0.111
9g	A + BC	Adams-Moulton	0.0557; 0.111
9h	CH_4 + T	Adams-Moulton	0.093-0.012
9i	$F + H_2$	Runge-Kutta-Gill	0.046
9j	M + XC(2D)	Adams-Moulton	0.0557; 0.111; 0.158
9k	M + XC(3D)	Adams-Moulton	0.37
9l	T + HR	Adams-Moulton	0.0186; 0.0557
9m	$F + H_2, HD, D_2$	Eleventh order Predictor-Corrector	0.014
	$^{18}F + HD$	Eleventh order Predictor-Corrector	0.002-0.014
9n	AB + CD	Adams-Moulton	0.0093
9o	A + BC	Adams-Moulton	0.0557

TABLE I (Continued)

Reference	System Studied	Integration Method	Stepsize (DT)*
9p	$F + H_2$	Other method**	0.028
9q	$H_2 + I$; $H_2 + Cl$ $HCl + H$	Runge-Kutta-Gill	0.04
9r	$H_2 + I_2$	Runge-Kutta-Gill Adams-Moulton Fifth order Predictor-Corrector Nordsieck's method	0.10 for four body systems 0.015-0.04 for three body systems
9s	$H + I_2$ $H + Br_2$	Runge-Kutta	0.025
9t	$H + I_2$	Runge-Kutta-Gill	0.046
9u	$H_2 + He$ $D_2 + He$	Runge-Kutta	0.50
9v	T + HR	Fourth order Predictor-Corrector	0.046
9w	$K + CH_3I$	Runge-Kutta	0.20
10	D + ClH $He + H_2^+$	Runge-Kutta-Gill	0.04

*Time in molecular units. See Table II.

**Reference 20a in Reference 9p.

TABLE II

RATIONAL MOLECULAR UNITS

Quantity	Unit
Energy	1 eV = 1.60210×10^{-12} erg
Distance	1 a.u = 0.529167×10^{-8} cm
Time	1 t.u = $0.53871469 \times 10^{-14}$ sec
Velocity	1 v.u = 0.9822769×10^{6} cm sec^{-1}
Momentum	1 mom.u = $1.631006453 \times 10^{-18}$ g.cm sec^{-1}

0.10 molecular units. Such a small stepsize requires large computer time, which is decidedly a factor against the quasiclassical trajectory study.

Recent studies (10) of the application of spline interpolation to the fitting of the potential-energy data indicated that even though trajectories with the same initial conditions do not match on the splinefitted and analytic surfaces, the average results on the spline-fitted surface are in excellent agreement with those obtained by using the analytic function. This suggests the possibility that an increase in integration step size may not alter the average results significantly so long as the total energy of the system is conserved. If this should prove to be the case, then the far more demanding criteria, such as back integration accuracy, could be dropped in quasiclassical scattering studies. Such a procedure would greatly increase the size of the integration step that could be employed and hence significantly reduce

the large computer time requirement. The present study reports the effect of changing the step size on the quasiclassical trajectory results such as differential cross section, total cross section and the distribution of translational energy partitioning fraction for D + ClH exchange reaction.

CHAPTER II

COMPUTATIONAL METHOD

The potential-energy surface (11) employed and the details of the computational procedure (1) have been described elsewhere.

The trajectories were computed by solving the twelve Hamiltonian Equations numerically using the Runge-Kutta-Gill procedure (1b) for a given set of initial conditions. The equations are of the general form

$$\frac{d\underset{\sim}{y}}{dt} = \underset{\sim}{f}[\underset{\sim}{y}(t)] \qquad \text{(II-1)}$$

where

$$y_i = Q_i,\ f_i = \frac{\partial H}{\partial P_i};\quad 1 \le i \le 6$$

$$y_i = P_i,\ f_i = -\frac{\partial H}{\partial Q_i};\quad 1 \le i \le 6$$

H is the Hamiltonian and the Q's and P's are the coordinates and the conjugate momenta in the center-of-mass coordinate system. If $\underset{\sim}{y}$ is known at time t_ν, then $\underset{\sim}{y}$ can be approximated at $t_\nu + h$ by

$$\underset{\sim}{y}(t_\nu + h) = \underset{\sim}{y}(t_\nu) + \int_{t_\nu}^{t_\nu + h} \underset{\sim}{f}[\underset{\sim}{y}(t)]dt \qquad \text{(II-2)}$$

The integral in the above equation can be replaced by the finite quadrature formula

$$\underset{\sim}{y}(t_\nu + h) = \underset{\sim}{y}(t_\nu) + h \sum_{i=0}^{\gamma-1} \omega_i \underset{\sim}{f}[\underset{\sim}{y}(t_\nu + \zeta_i h)] \qquad \text{(II-3)}$$

where h is the integration stepsize, γ the order of the method, ζ_i's are quadrature points such that $0 \leq \zeta_i \leq 1$, and ω_i's the weighting parameters. The above equation requires the function values at the intermediate times $(t_\nu + \zeta_i h)$ which can be approximated by

$$\underset{\sim}{y}(t_\nu + \zeta_i h) = \underset{\sim}{y}(t_\nu) + h \sum_{j=0}^{i-1} w_{ij} \underset{\sim}{f}[\underset{\sim}{y}(t_\nu + \zeta_j h)] \qquad \text{(II-4)}$$

For a quadrature of degree r, there are thus $(1/2)r(r+3)$ parameters ζ_i, ω_i and w_{ij}, to be determined. So, for the fourth order Runge-Kutta-Gill procedure, 14 parameters are needed and are listed in Table III. In the present calculation, the integration stepsize (h = DT) was varied from 0.02 to 0.40 molecular units. For DT = 0.30, 5000 trajectories were computed while for all other stepsizes, only 500 were examined. The results for DT = 0.02 have previously been reported by Raff et al. (2). These results involve the examination of 3049 trajectories.

All calculations were carried out at a single relative velocity equal to 6.050×10^5 cm/sec, for a velocity selected beam of deuterium atoms interacting with a hydrogen chloride beam at 250K.

TABLE III

PARAMETERS FOR THE 4th-ORDER RUNGE-KUTTA-GILL METHOD[a]

i	0	1	2	3
ζ_i	0	1/2	1/2	1
ω_i	1/6	$1/3(1-\sqrt{1/2})$	$1/3(1+\sqrt{1/2})$	1/6
w_{io}		1/2	$-1/2+\sqrt{1/2}$	0
w_{i1}			$1-\sqrt{1/2}$	$-\sqrt{1/2}$
w_{i2}				$1+\sqrt{1/2}$

[a]Reference 1b.

CHAPTER III

RESULTS AND DISCUSSIONS

Tables IV and V compare the initial coordinates (Q_i) and the conjugate momenta for the D + ClH system in the center-of-mass coordinate frame, with the backintegrated conditions for a typical nonreactive and a reactive trajectory for different step sizes. Total energies of the system at the beginning, end and after backintegration of a reactive and a nonreactive trajectory are listed in Table VI. Figure 1-5 compare the distribution of translational energy partitioning fraction for different step sizes. The differential cross section is plotted as a function of center-of-mass scattering angle in Figures 6-10. The average translational partitioning fraction ($\langle f_t \rangle$) and the cross section (S) computed for the exchange reaction

$$D + ClH \longrightarrow DCl + H$$

are listed in Table VII.

In most of the quasiclassical trajectory studies, the accuracy of the backintegrated results to three or four significant digits has been the criterion for the choice of step size. In Table IV the backintegrated results for the step size 0.02 are accurate to two significant digits or even less. In order to obtain three significant digit accuracy for all Q_i and P_i, the step size must be even smaller than 0.02 molecular units. This would result in a large increase in the

TABLE IV

INITIAL AND THE BACKINTEGRATED COORDINATES AND CONJUGATE MOMENTA FOR A TYPICAL NONREACTIVE TRAJECTORY

Step Size	Q_1[a]	Q_2	Q_3	Q_4	Q_5	Q_6	P_1	P_2	P_3	P_4	P_5	P_6
						Initial Conditions[b]						
	2.1107	-1.4555	0.2886	0.0	3.1260	-7.3640	0.2891	-0.2528	-0.0075	0.0	0.0	1.1767
						Backintegrated Results						
0.02	2.1118	-1.4541	0.2850	-0.0014	3.1273	-7.3577	0.2892	-0.2525	-0.0079	0.0003	-0.0006	1.1751
0.04	2.1113	-1.4547	0.2868	-0.0006	3.1268	-7.3607	0.2891	-0.2526	-0.0077	0.0001	-0.0004	1.1759
0.08	2.1108	-1.4549	0.2878	-0.0002	3.1266	-7.3622	0.2892	-0.2528	-0.0076	0.0000	-0.0002	1.1762
0.10	2.1102	-1.4547	0.2881	-0.0002	3.1267	-7.3625	0.2893	-0.2529	-0.0076	0.0000	-0.0002	1.1763
0.12	2.1091	-1.4542	0.2884	-0.0002	3.1271	-7.3629	0.2896	-0.2532	-0.0075	0.0000	-0.0003	1.1764
0.16	2.1036	-1.4514	0.2895	-0.0005	3.1291	-7.3636	0.2909	-0.2542	-0.0073	0.0001	-0.0006	1.1765
0.20	2.0904	-1.4443	0.2917	-0.0010	3.1341	-7.3649	0.2926	-0.2558	-0.0071	0.0003	-0.0016	1.1766
0.30	2.0204	-1.4049	0.3020	-0.0039	3.1589	-7.3698	0.2455	-0.2249	-0.0144	0.0013	-0.0061	1.1769
0.40	1.9777	-1.3741	0.2999	-0.0045	3.1624	-7.3693	0.0695	-0.1035	-0.0419	0.0015	-0.0066	1.1764

[a] The Q_i and P_i are defined in Reference 3.

[b] All units are rational molecular units defined in Table II.

TABLE V

INITIAL AND THE BACKINTEGRATED COORDINATES AND CONJUGATE MOMENTA FOR A TYPICAL REACTIVE TRAJECTORY

Step Size	Q_1[a]	Q_2	Q_3	Q_4	Q_5	Q_6	P_1	P_2	P_3	P_4	P_5	P_6
						Initial Conditions[b]						
	2.1744	-0.1514	-0.9443	0.0	3.1202	-7.3664	0.5122	-0.0647	-0.2957	0.0	0.0	1.1767
						Backintegrated Results						
0.02	2.1814	-0.1372	-0.9293	0.0122	3.1345	-7.3457	0.5128	-0.0624	-0.2933	-0.0014	-0.0023	1.1734
0.04	2.1781	-0.1436	-0.9365	0.0064	3.1264	-7.3553	0.5125	-0.0634	-0.2944	-0.0007	-0.0009	1.1749
0.08	2.1762	-0.1474	-0.9403	0.0032	3.1231	-7.3608	0.5121	-0.0640	-0.2950	-0.0004	-0.0005	1.1757
0.10	2.1758	-0.1482	-0.9412	0.0026	3.1221	-7.3619	0.5116	-0.0641	-0.2949	-0.0003	0.0003	1.1759
0.12	2.1753	-0.1486	-0.9416	0.0022	3.1217	-7.3626	0.5104	-0.0641	-0.2945	-0.0002	-0.0002	1.1760
0.16	2.1741	-0.1488	-0.9418	0.0018	3.1202	-7.3635	0.5046	-0.0638	-0.2921	-0.0002	-0.0000	1.1762
0.20	2.1714	-0.1483	-0.9414	0.0016	3.1179	-7.3642	0.4896	-0.0627	-0.2858	-0.0002	0.0003	1.1764
0.30	2.1604	-0.1359	-0.9407	0.0050	3.0845	-7.3610	0.3772	-0.0542	0.2374	-0.0010	0.0061	1.1761
0.40	2.2868	-0.1019	-0.5179	0.0937	3.6966	-7.3837	-0.0835	-0.0225	-0.0939	-0.0016	-0.0969	1.1825

[a] The Q_i and P_i are defined in Reference 3.

[b] All units are rational molecular units defined in Table II.

TABLE VI

INITIAL, FINAL AND BACKINTEGRATED VALUES OF THE TOTAL ENERGY OF THE SYSTEM FOR A TYPICAL NONREACTIVE AND A REACTIVE TRAJECTORY

Step Size[a]	Initial E(eV)	Final E(eV)	Backintegrated E(eV)
	NONREACTIVE TRAJECTORY		
0.02	-4.079171	-4.079566	-4.079914
0.04	-4.079171	-4.079396	-4.079588
0.08	-4.079171	-4.079409	-4.079633
0.10	-4.079171	-4.079632	-4.080035
0.12	-4.079171	-4.080126	-4.081016
0.16	-4.079171	-4.082829	-4.086187
0.20	-4.079171	-4.089590	-4.098753
0.30	-4.079171	-4.138118	-4.173390
0.40	-4.079171	-4.217207	-4.243596
	REACTIVE TRAJECTORY		
0.02	-4.076887	-4.078194	-4.079485
0.04	-4.076887	-4.077587	-4.078285
0.08	-4.076887	-4.077294	-4.077746
0.10	-4.076887	-4.077403	-4.077905
0.12	-4.076887	-4.077652	-4.078495
0.16	-4.076887	-4.079449	-4.081973
0.20	-4.076887	-4.083645	-4.090248
0.30	-4.076887	-4.118822	-4.148996
0.40	-4.076887	-4.191640	-4.227419

[a]Rational molecular units. See Table II.

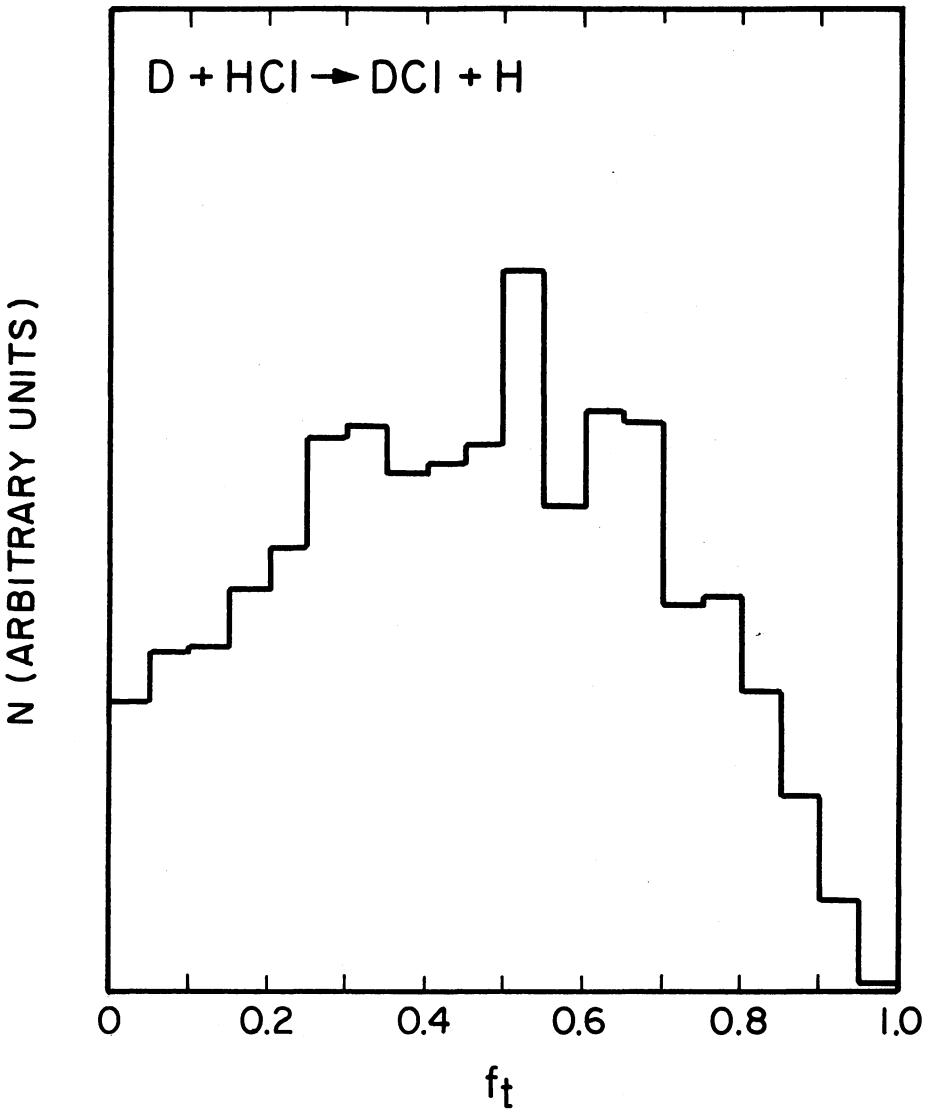

Figure 1. Energy Partitioning Distribution for the D + HCl Exchange Reaction. f_t is the Fraction of the Total Available Energy Partitioned into Relative Translational Motion of the Products

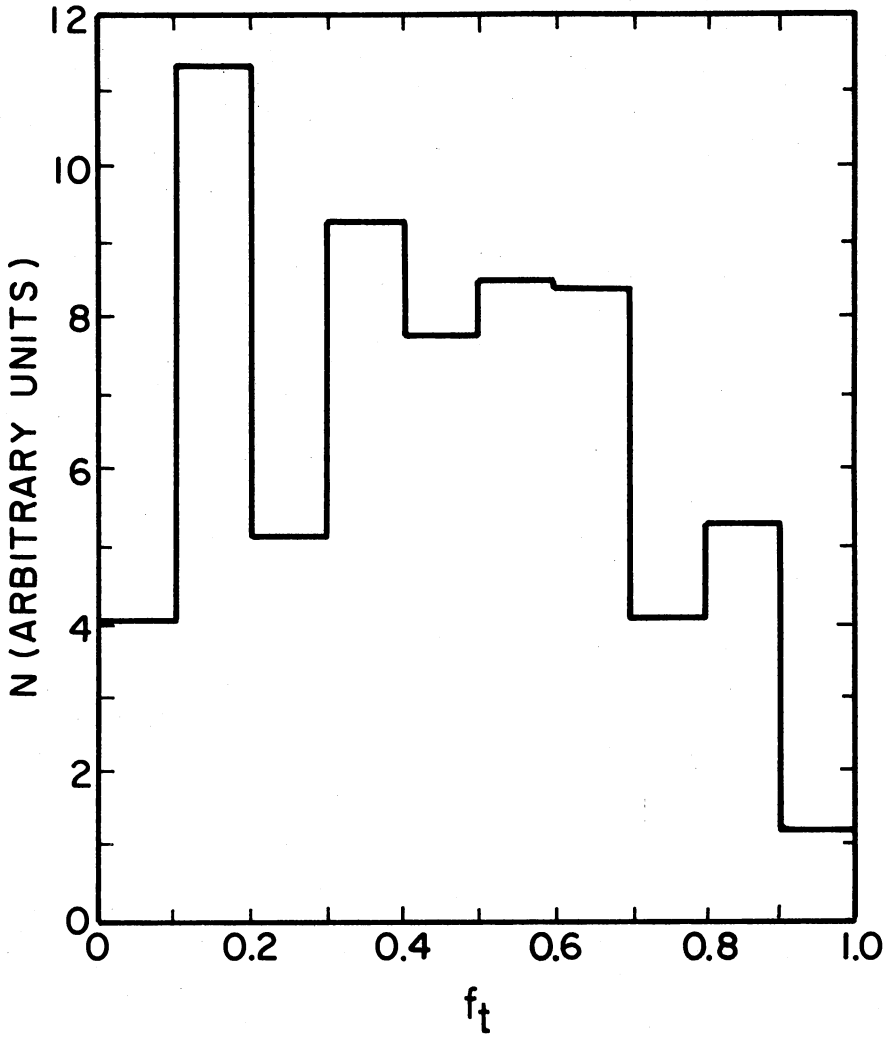

Figure 2. Energy Partitioning Distribution for the D + ClH Exchange Reaction Using DT = 0.16. f_t is the Fraction of the Total Available Energy Partitioned into Relative Translational Motion of the Products

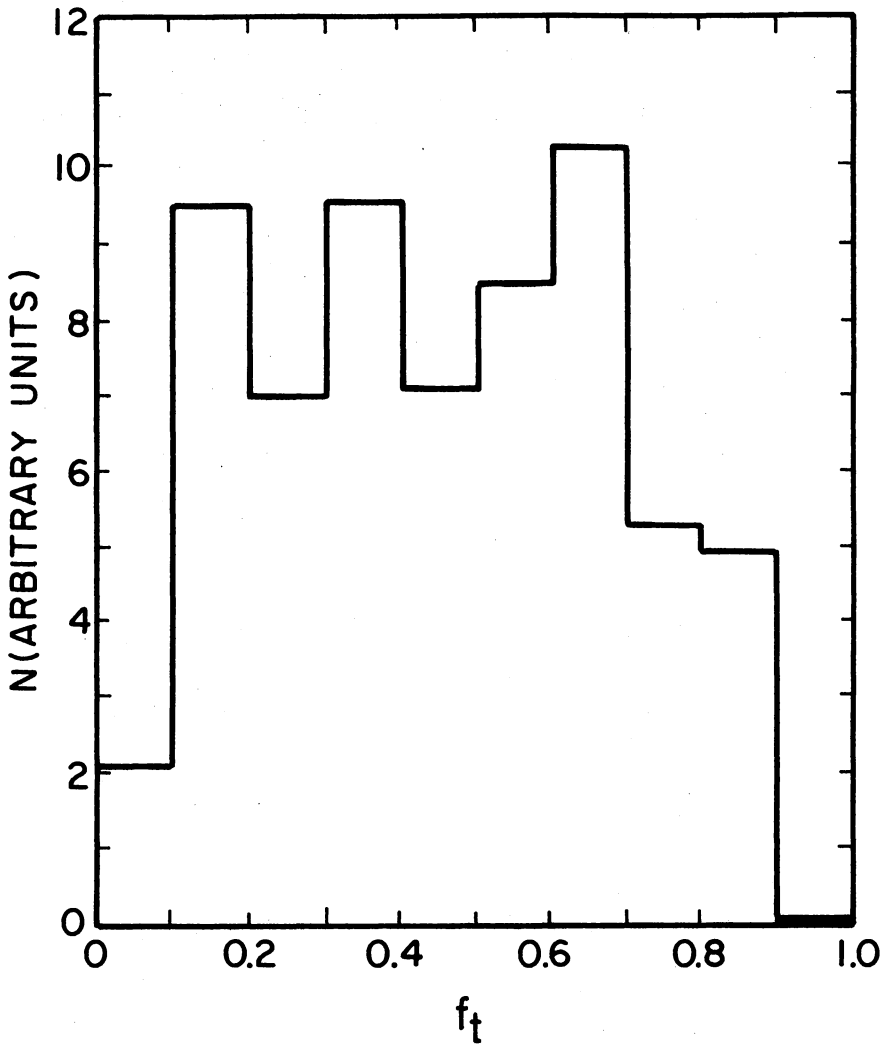

Figure 3. Energy Partitioning Distribution for the D + ClH Exchange Reaction Using DT = 0.20. f_t is the Fraction of the Total Available Energy Partitioned into Relative Translational Motion of the Products

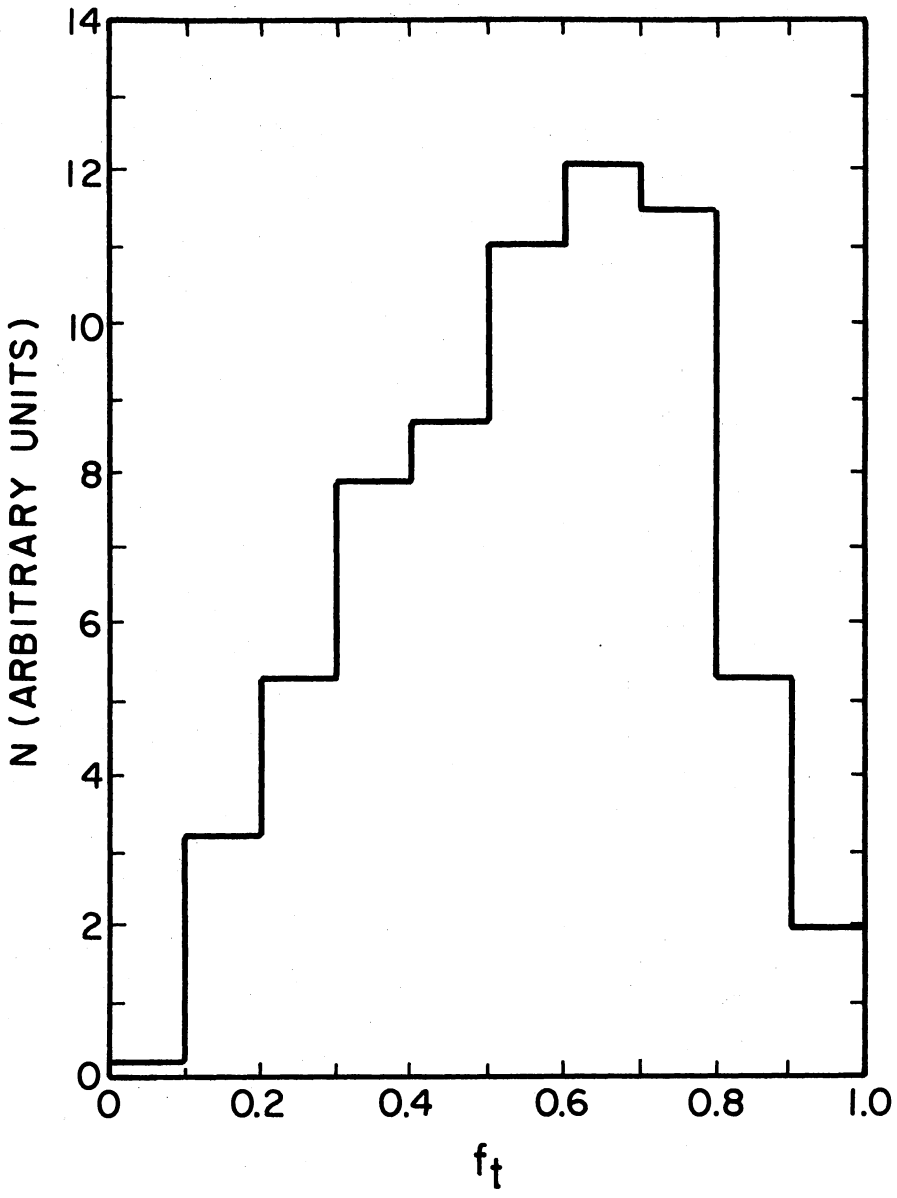

Figure 4. Energy Partitioning Distribution for D + ClH Exchange Reaction Using DT = 0.30. f_t is the Fraction of the Total Available Energy Partitioned into Relative Translational Motion of the Products

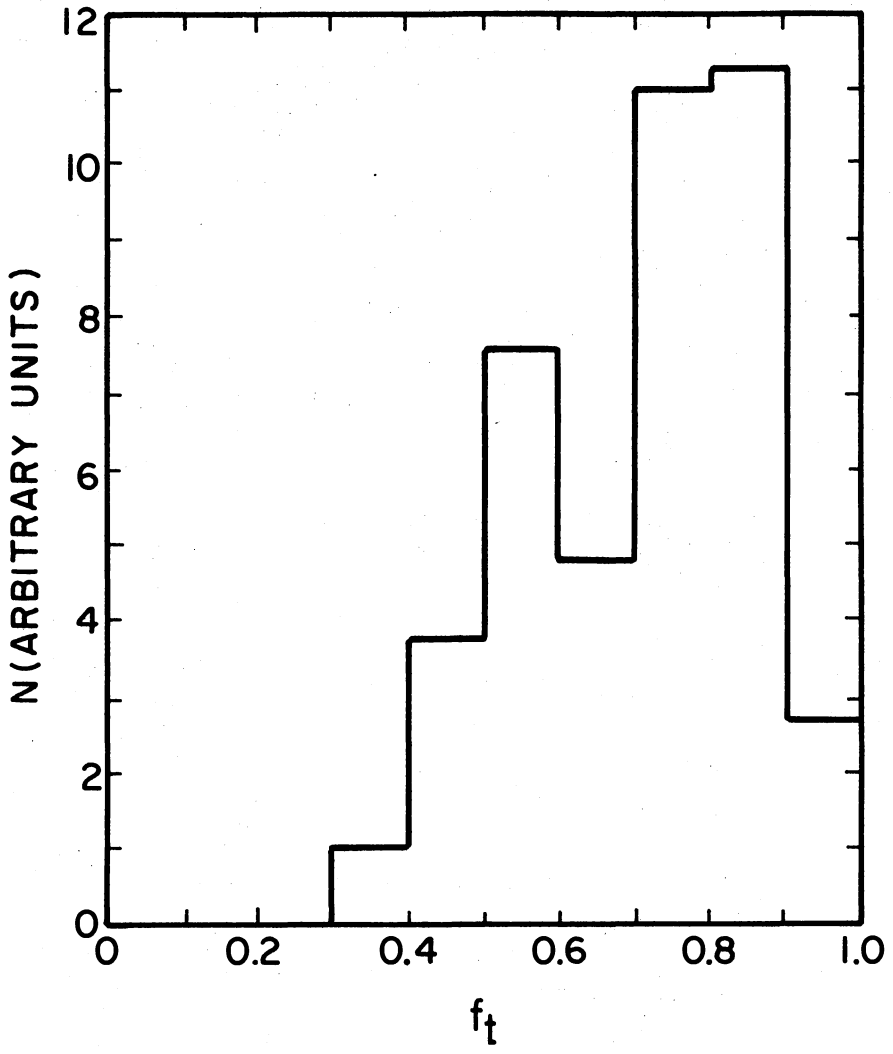

Figure 5. Energy Partitioning Distribution for D + ClH Exchange Reaction Using DT = 0.40. f_t is the Fraction of the Total Available Energy Partitioned into Relative Translational Motion of the Products

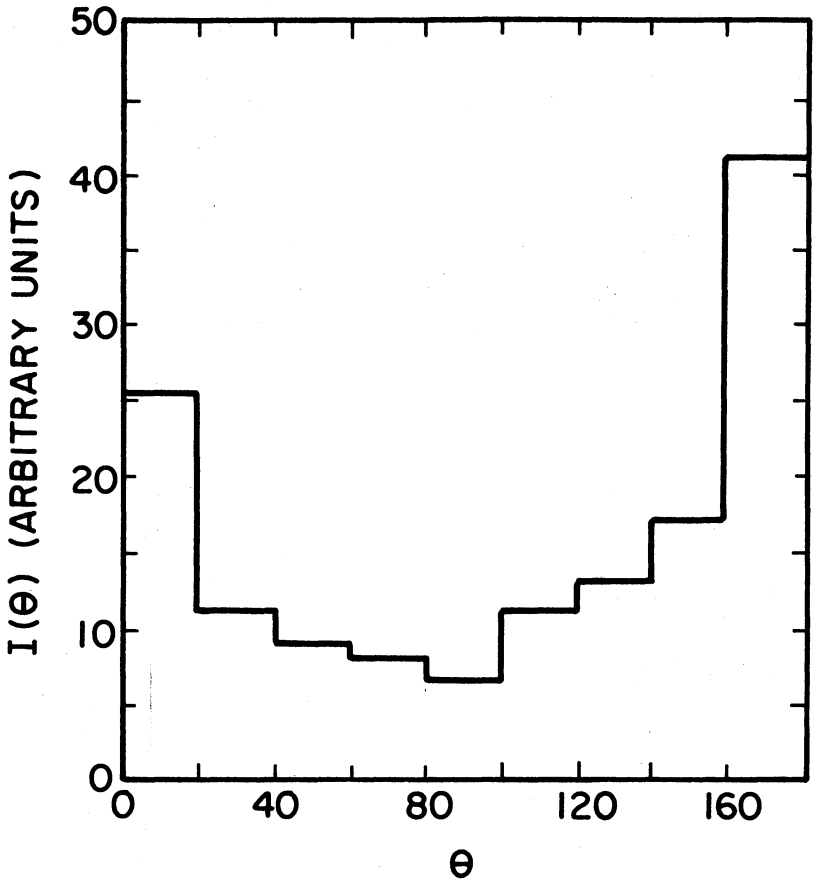

Figure 6. Center of Mass Differential Scattering Cross Section for DC1 Scattering Using DT = 0.02

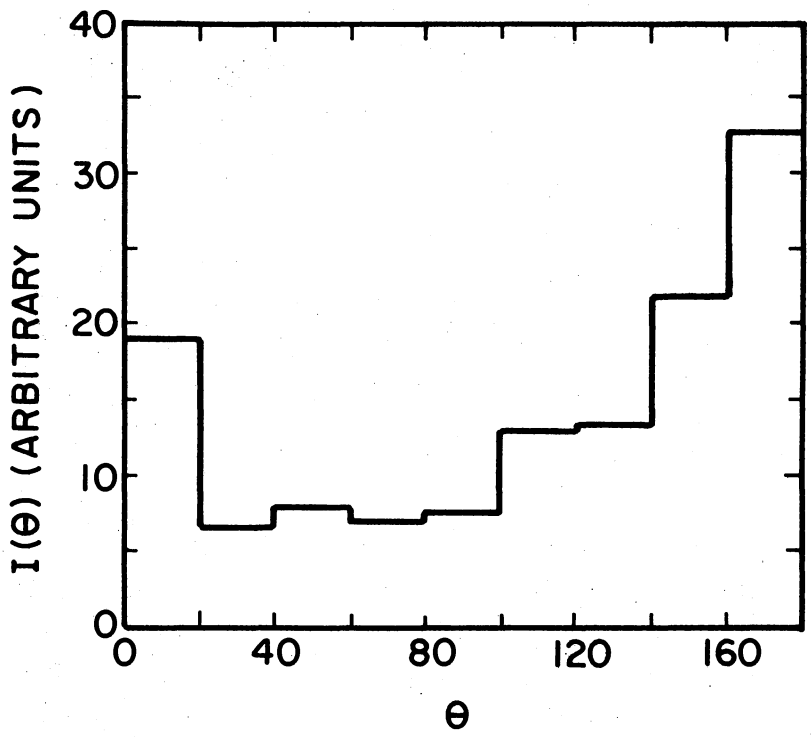

Figure 7. Center of Mass Differential Scattering Cross Section for DC1 Scattering Using DT = 0.16

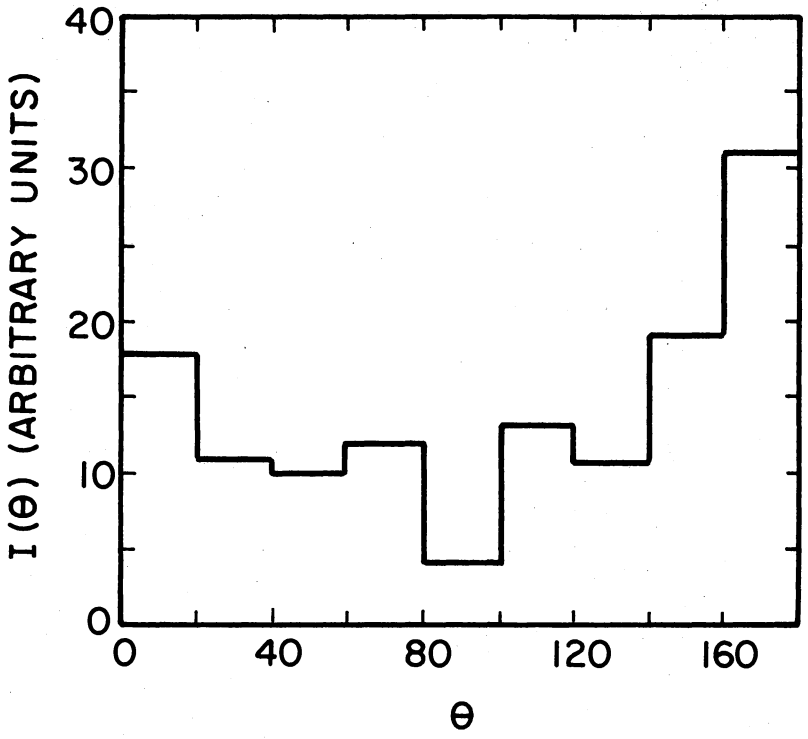

Figure 8. Center of Mass Differential Scattering Cross Section for DC1 Scattering Using DT = 0.20

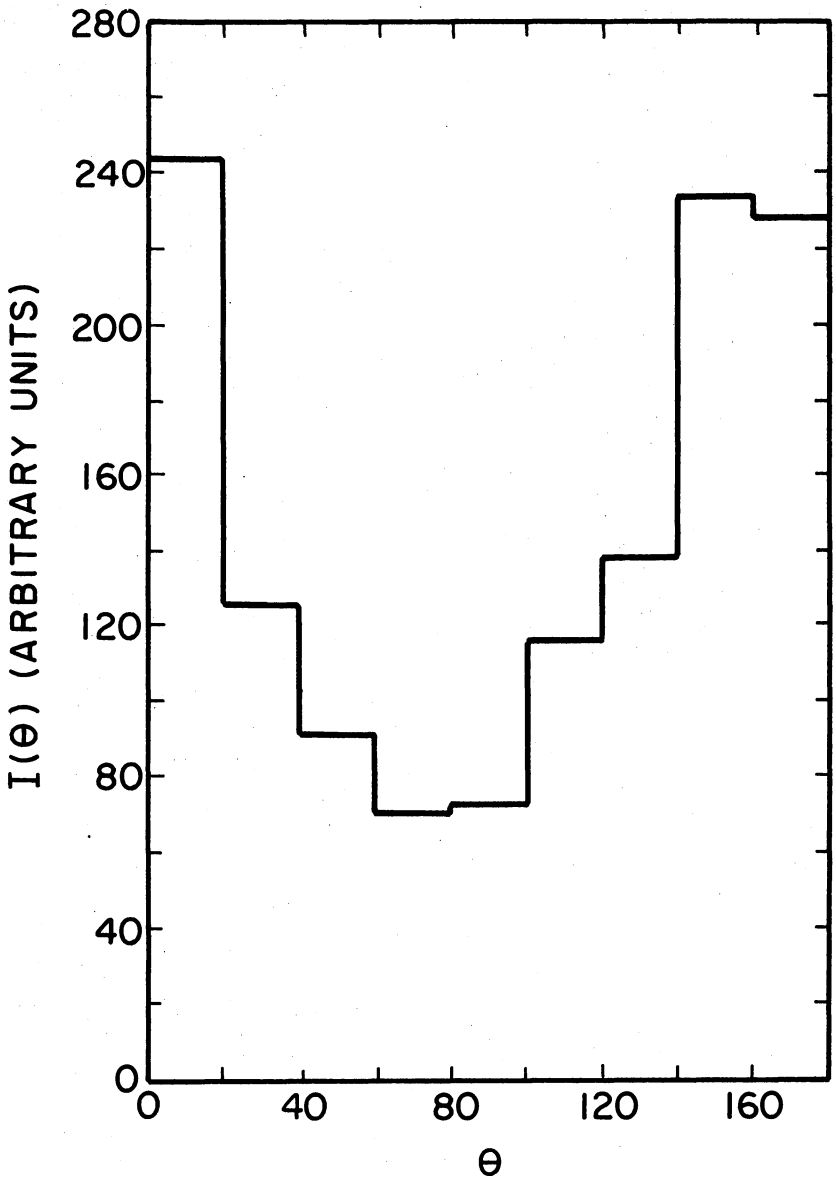

Figure 9. Center of Mass Differential Scattering Cross Section for DC1 Scattering Using DT = 0.30

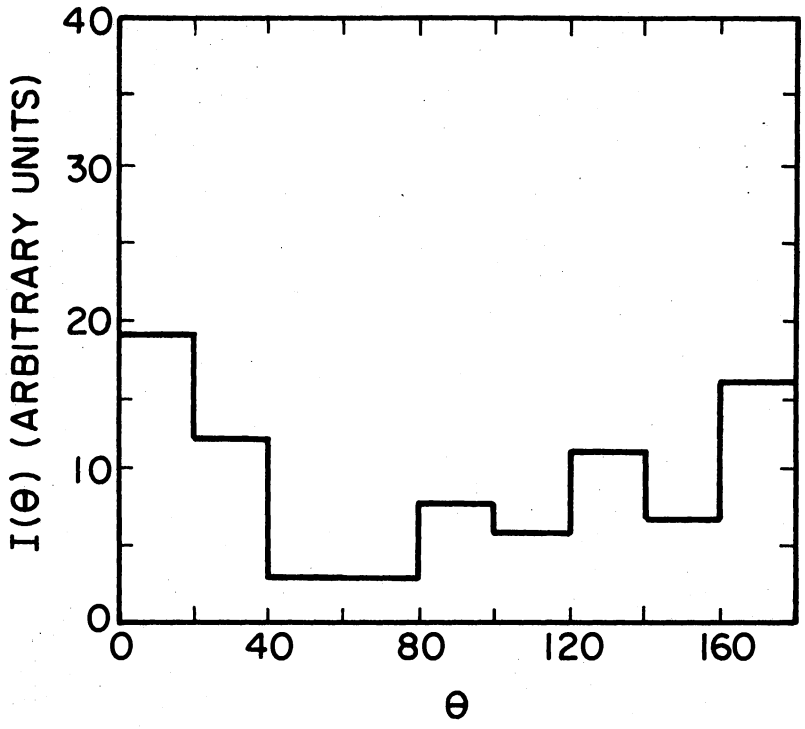

Figure 10. Center of Mass Differential Scattering Cross Section for DC1 Scattering Using DT = 0.40

TABLE VII

COMPARISON OF AVERAGE RESULTS FOR DIFFERENT STEPSIZES (DT). $\langle f_t \rangle$ IS THE AVERAGE TRANSLATIONAL ENERGY PARTITIONING DISTRIBUTION FRACTION AND S IS THE COMPUTED TOTAL CROSS SECTION FOR THE EXCHANGE REACTION

DT in Molecular Units	$\langle f_t \rangle$	S(au^2)
0.02[a]	0.46	3.38 ± 0.11
0.16	0.43	3.65 ± 0.30
0.20	0.46	3.65 ± 0.30
0.30[b]	0.54	3.76 ± 0.10
0.40	0.69	2.41 ± 0.24

[a]Result of 3049 trajectories. See Reference 3.

[b]Result of 5000 trajectories

required computer time. On the other hand, the total energy of the system for a reactive trajectory (Table VI) is conserved to three significant digits even for larger step sizes. As the step size increases, the extent of the energy conservation decreases, resulting in an error in the first significant digit for DT = 0.40 molecular units.

The crucial question, however, is not the accuracy of back-integrated Q_i and P_i or energy conservation, but rather the accuracy of the computed distribution. The energy partitioning distribution plot in Figure 1 is the result of 3049 trajectories obtained by Raff et al. (2). As the step size is increased 8 times, the distribution is

distorted but the main features still remain the same. With further increase in step size the distribution is distorted further and hence the average translational energy partitioning distribution fraction remains approximately constant only up to DT = 0.2. The distribution plots of center-of-mass differential scattering cross section in Figure 6-8 are approximately the same for a ten fold increase in step size, showing a predominantly backward scattering and a significant but less forward scattering of DCl. With further increase in step size, the distribution changes significantly. However the total reaction cross section (S) for the exchange reaction, as illustrated in Table VII is identical for step sizes ranging from 0.02-0.30 molecular units. Only at DT = 0.40 (a twenty-fold increase in step size) does it become significantly different.

Conclusions

It is clear from the above results that a large increase, as high as fifteen fold, in step size may not yield accurate energy distributions but would result in reasonably accurate differential cross sections, average translational energy partitioning distribution fractions and accurate total reaction cross sections. The main criterion seems to be the conservation of the total energy of the system rather than the more demanding criteria of backintegration accuracy. If the aim of a quasiclassical trajectory study is to compute the total reaction cross section and averages of other experimentally measurable quantities, a large step size could be used. This would result in enormous savings in computer time as shown in Table VIII for the D + ClH system. It is important to

note that the savings is not significant for DT > 0.16 when the results become less accurate.

TABLE VIII

COMPARISON OF COMPUTING TIME PER TRAJECTORY (T) ON AN IBM 360/65 COMPUTER FOR DIFFERENT STEPSIZES

DT[a]	T in seconds
0.02	12.01
0.16	1.55
0.20	1.26
0.30	0.92

[a]In molecular units.

PART II

STUDY OF THE ROLE OF VIBRATIONAL ENERGY IN REACTIVE COLLISIONS: $He + H_2^+ \rightarrow HeH^+ + H$ USING SPLINEFITTED *AB INITIO* AND DIM POTENTIAL-ENERGY SURFACES

CHAPTER IV

INTRODUCTION

Recent success in the use of chemical lasers for separating isotopes (12) has provided a stimulus to the understanding of the role of vibrational energy in chemical reactions. From the theoretical point of view, several systems (13) have been studied, mostly by the quasi-classical trajectory (QCT) method, and it has been found that vibrational energy is more effective than translational energy for endoergic reactions whenever the potential-energy barrier lies in the exit channel. Experimentally, chemiluminescence studies (14) have provided indirect information on the effect of increasing vibrational energy on the reaction rate of endoergic reactions of neutral species while photoionization studies, because of the ease of selection of vibrational states, have provided direct information on the same aspect of the problem for ion-molecule reactions (15) (16).

Photoionization studies of the $He + H_2^+(v = 0\text{-}5) \rightarrow HeH^+ + H$ reaction by Chupka and coworkers (16a) showed that for the same total energy the reaction cross section increases with increase in the vibrational state of the hydrogen molecular ion for a wide range of total system energy (1.0-4.0 eV). Due to its simplicity, this system provides an unique opportunity to test the existing theoretical approaches. Brown and Hayes (17) computed the potential-energy surface for the collinear HeH_2^+ configuration using LCAO-MO-SCF methods. Kuntz (18) provided a

Diatomics-In-Molecule (DIM) analytic function to fit the results of Brown and Hayes (17). Using the DIM function, two independent quantum mechanical studies (19) (20) and one QCT study (21) have been made on this system and the results are given in Figures 11 and 12. Figures 13 through 15 compare the results from quantal and classical calculations for $v = 0$, 1 and 2 states. They are in excellent agreement with each other but in complete contrast with the experimental findings (16a) as illustrated in Figure 16, in that the theoretical results indicate an absence of vibrational enhancement. These results are also in conflict with earlier theoretical studies (13).

It has recently (22) been shown that small changes in a potential energy surface can lead to significant changes in the final results. Hence it is possible that this anomaly in the theoretical investigations for this system could be due to the inadequacy of the DIM function in fitting the ab initio surface of Brown and Hayes (BH) and that a better fit to the ab initio surface could lead to results in accord with experiment. A cubic spline interpolation procedure (23) has recently proved to be a valuable tool in the interpolation of ab initio potential-energy surfaces. The results of using such a splinefitting procedure on the Brown and Hayes ab initio surface and the subsequent QCT studies are reported here.

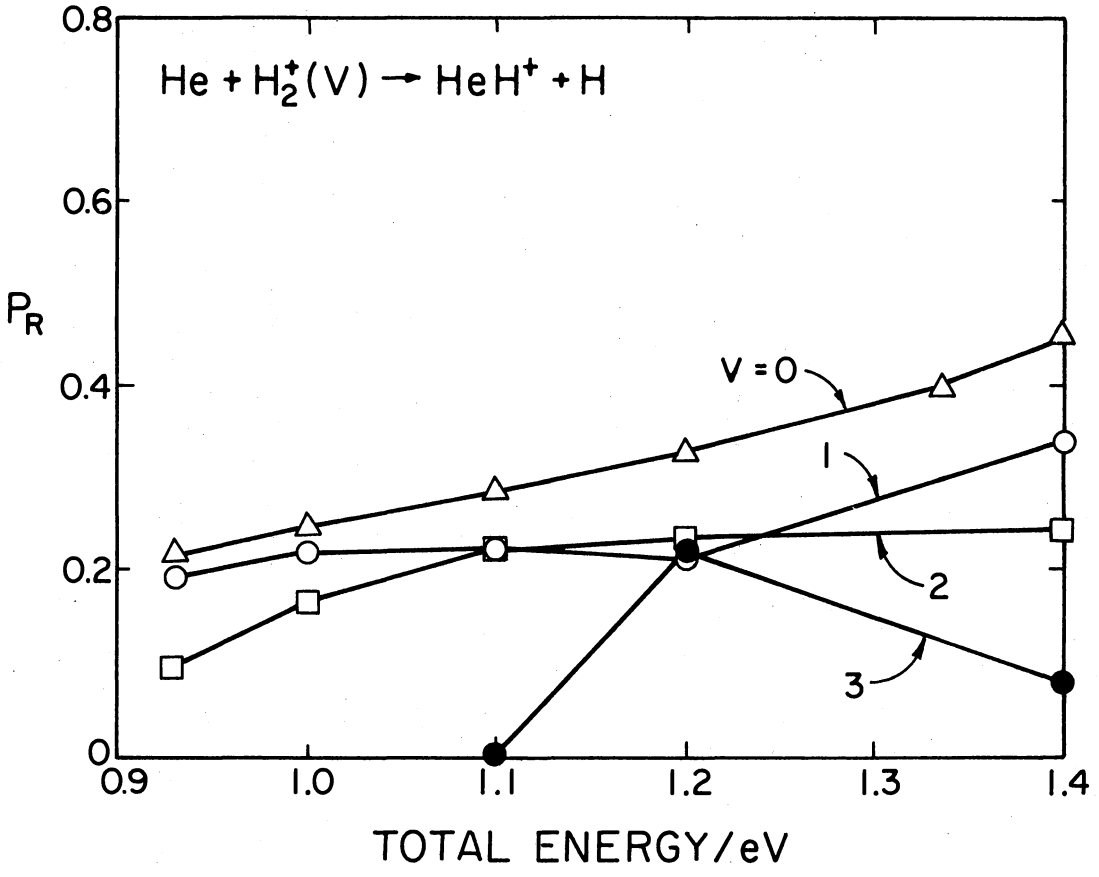

Figure 11. Quasiclassical Reaction Probability as a Function of Total Energy of the System for Different Vibrational States

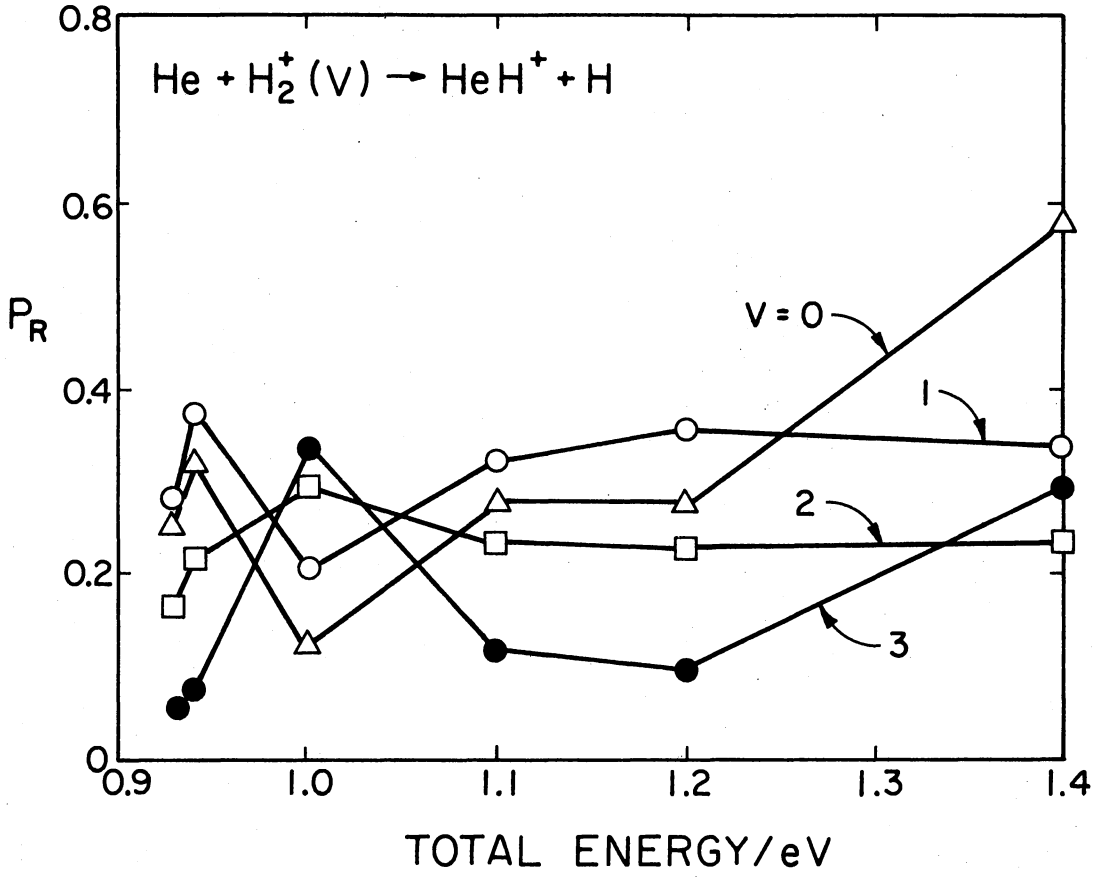

Figure 12. Quantum Mechanical Reaction Probabilities (19a) as a Function of Total Energy of the System for Different Vibrational States

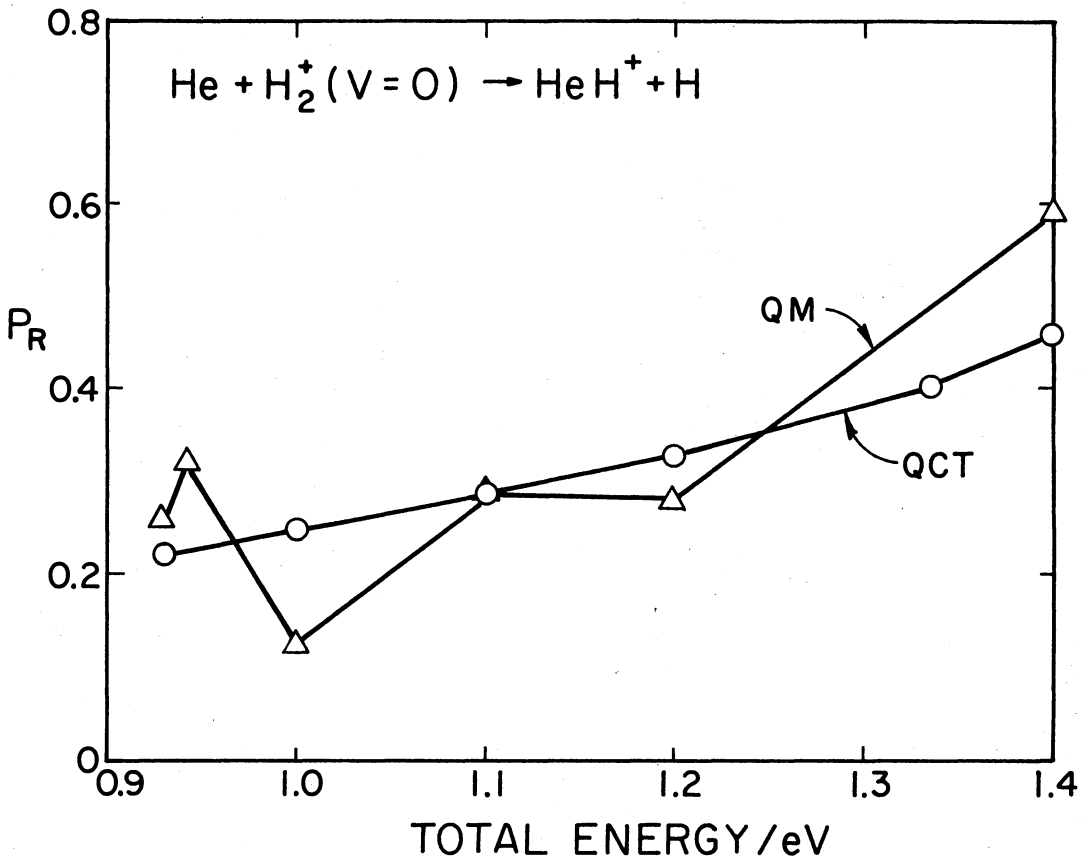

Figure 13. Comparison of Quasiclassical and Quantum Mechanical Reaction Probabilities (19a) for v = 0 State of H_2^+

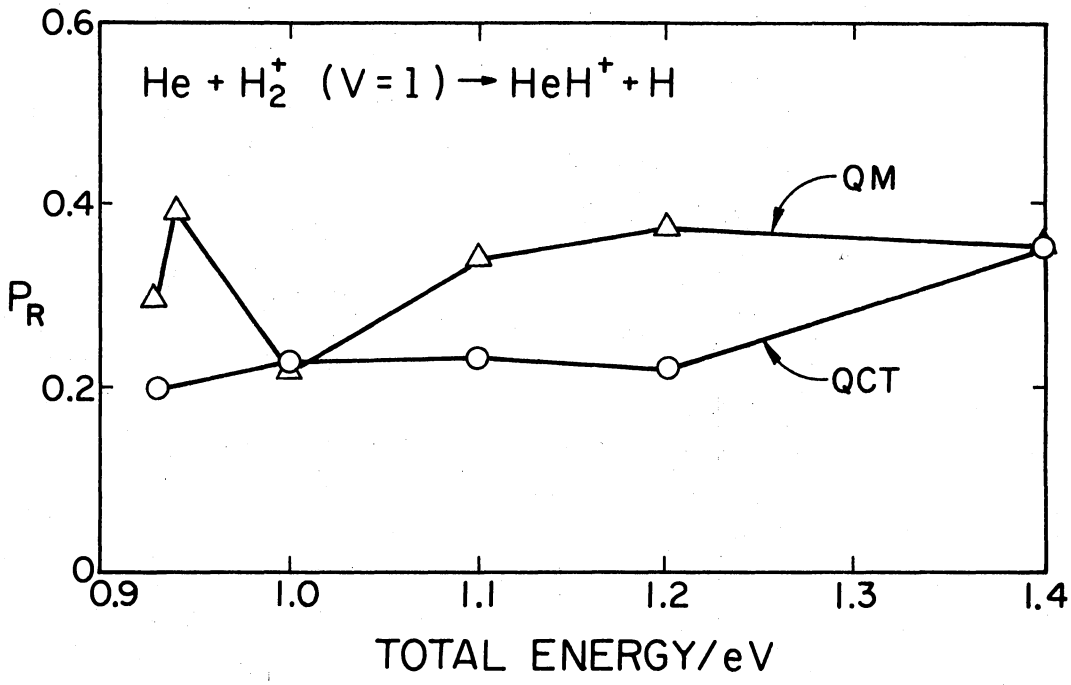

Figure 14. Comparison of Quasiclassical and Quantum Mechanical (19a) Reaction Probabilities for v = 1 State of H_2^+

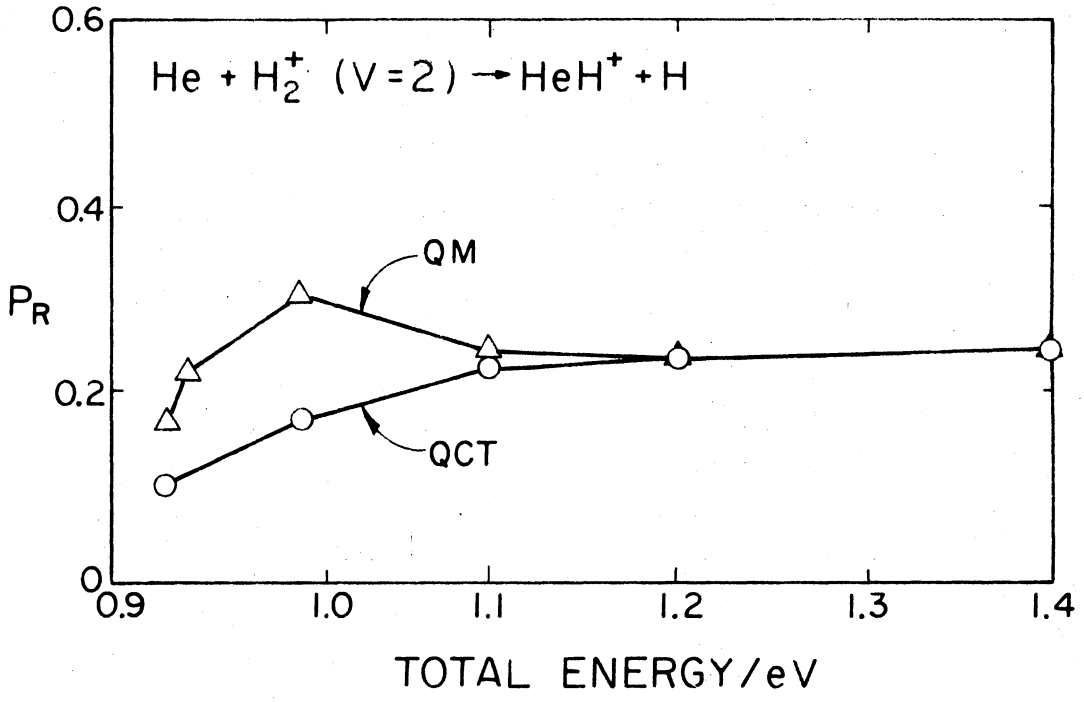

Figure 15. Comparison of Quasiclassical and Quantum Mechanical (19a) Reaction Probabilities for v = 2 State of H_2^+

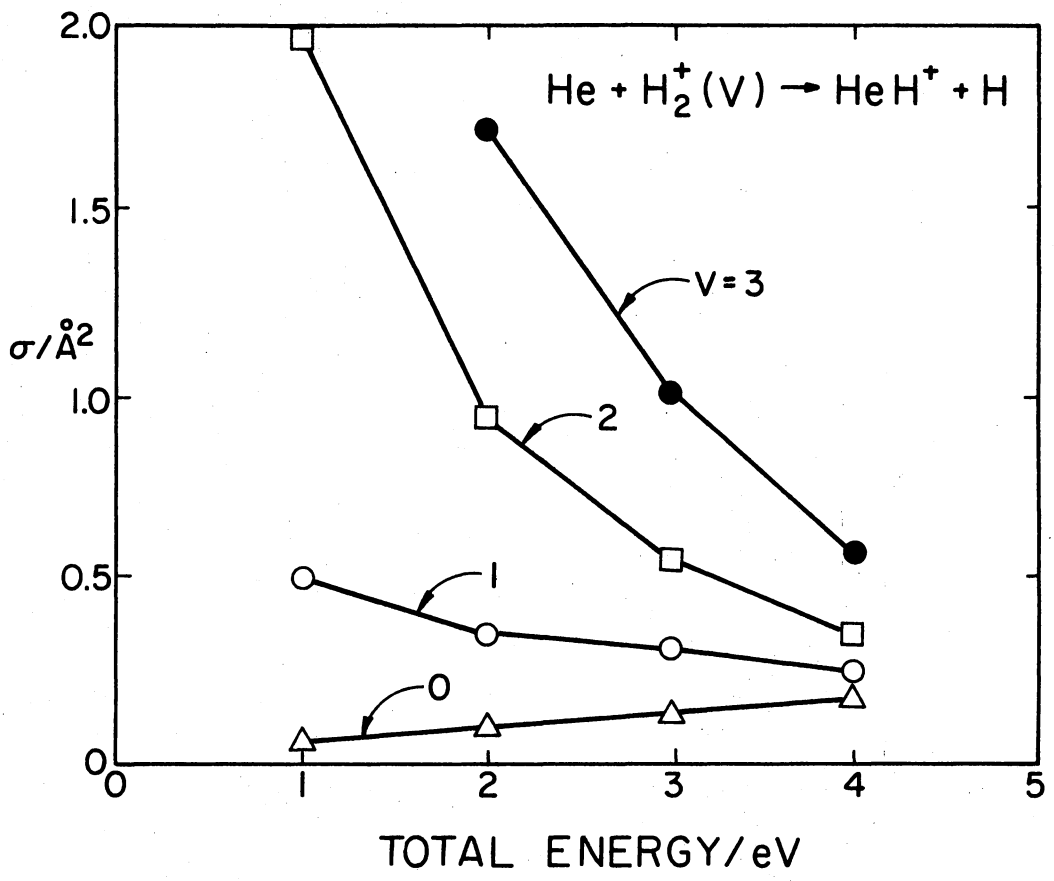

Figure 16. Experimental Reaction Cross Section as a Function of Total Energy of the System for Different Vibrational States

CHAPTER V

COMPUTATIONAL PROCEDURE

Brown and Hayes (17) reported the potential-energy values for a range of R_1 and R_2 values (see Figure 17). However these values are not reported for a complete rectangular grid of R_1 and R_2. The spline interpolation procedure requires the potential-energy values for a rectangular grid of R_1 and R_2. Table IX gives the energy values relative to the isolated He + H_2^+ configuration for a 12 x 16 grid of R_1 and R_2. The values in parentheses were obtained by one dimensional spline interpolation or graphical extrapolation of the remaining values in the appropriate row or column. For $R_1 > 3.6$ there are no values reported by Brown and Hayes (17). Values in this region were computed from the DIM function (18), as such functions are known to be accurate in the reactant and product regions because of the Morse curve fit to diatomic molecule energy. Also, the accuracy of the potential-energy values is more important in the interaction region than in the separated reactant or product regions. Potential-energy contours obtained by interpolating (the details of the procedure have been described elsewhere (23a)) the set of 12 x 16 values are plotted in Figure 18. This is referred to as the splinefitted ab initio (SAI) surface. For comparison, Figure 19 shows the potential-energy contours obtained using the DIM function. The method used for the QCT study is the same as that of Karplus, Porter and Sharma (1a) except that the

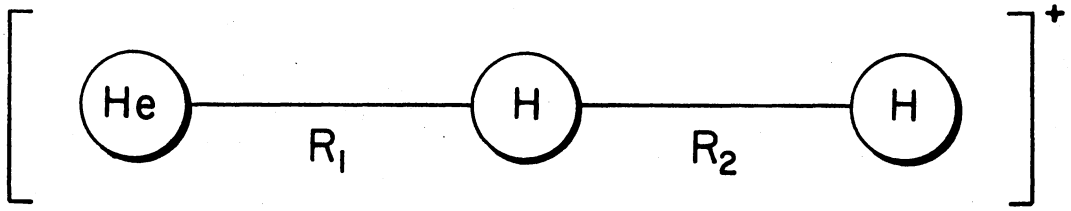

Figure 17. Internuclear Distances for Collinear $HeHH^+$ Configuration

TABLE IX

POTENTIAL-ENERGY VALUES IN eV RELATIVE TO THE He + H_2^+ ASYMPTOTIC LIMIT

R_2/R_1	1.4	1.6	1.8	2.0	2.4	2.8
1.4	(1.53749)	(1.19701)	0.97089	0.83818	0.76826	0.78205
1.6	1.09681	0.58539	0.34591	0.24054	0.19248	0.21062
1.8	0.65994	0.22175	0.02956	-0.04697	-0.06890	-0.04352
2.0	0.41735	0.04539	-0.10168	-0.14919	-0.14297	-0.10881
2.2	(0.29675)	(-0.01643)	-0.12065	-0.13967	-0.10435	-0.06052
2.4	0.25321	-0.00677	-0.07202	-0.06335	0.00151	0.05559
2.8	(0.28554)	0.11826	0.12436	0.18592	0.31015	(0.38099)
3.2	0.39550	0.29284	0.35987	0.47039	0.65460	0.75360
3.6	(0.51246)	0.46149	0.57877	0.73378	0.97915	(1.10597)
4.0	0.61448	0.60155	0.75833	0.95169	(1.25786)	1.41518
4.4	(0.69461)	0.70777	0.89330	1.11728	1.48112	(1.67267)
4.8	(0.75410)	0.78358	(0.98833)	(1.23458)	(1.64599)	1.87883
5.2	(0.79663)	(0.83584)	1.05235	(1.31254)	1.76072	(2.03628)
5.6	(0.82580)	0.86997	(1.09450)	(1.36024)	(1.83648)	(2.14499)
6.0	0.84521	(0.89133)	1.12048	(1.38682)	1.88039	2.20441
6.8	0.86691	0.91676	1.14799	(1.41383)	(1.90486)	(2.23683)

R_2/R_1	3.6	4.0	5.0	6.0	7.0	8.0
1.4	(0.66924)	0.68539	0.70155	0.70529	0.70613	0.70632
1.6	0.26372	0.25316	0.26892	0.27256	0.27337	0.27356
1.8	0.00991	0.04036	0.05584	0.05940	0.06020	0.06038
2.0	-0.05377	-0.01979	-0.00449	-0.00098	-0.00019	-0.00002

TABLE IX (Continued)

R_2/R_1	3.6	4.0	5.0	6.0	7.0	8.0
2.2	(-0.00275)	0.02363	0.03884	0.04231	0.04309	0.04326
2.4	0.11574	0.13480	0.14997	0.15341	0.15418	0.15435
2.8	(0.44232)	0.46409	0.47934	0.48276	0.48352	0.48369
3.2	0.82730	0.83841	0.85389	0.85730	0.85806	0.85823
3.6	(1.21017)	1.19562	1.21148	1.21491	1.21566	1.21583
4.0	1.50900	1.50976	1.52617	1.52962	1.53038	1.53055
4.4	(1.75291)	1.17735	1.79066	1.79414	1.79490	1.79507
4.8	(1.96570)	1.98853	2.00666	2.01020	2.01097	2.01113
5.2	(2.13458)	2.16030	2.17974	2.18335	2.18412	2.18429
5.6	(2.26602)	2.29544	2.31659	2.32031	2.32108	2.32125
6.0	(2.36633)	2.40039	2.42378	2.42762	2.42840	2.42857
6.8	(2.54433)	2.54165	2.57161	2.57585	2.57665	2.57682

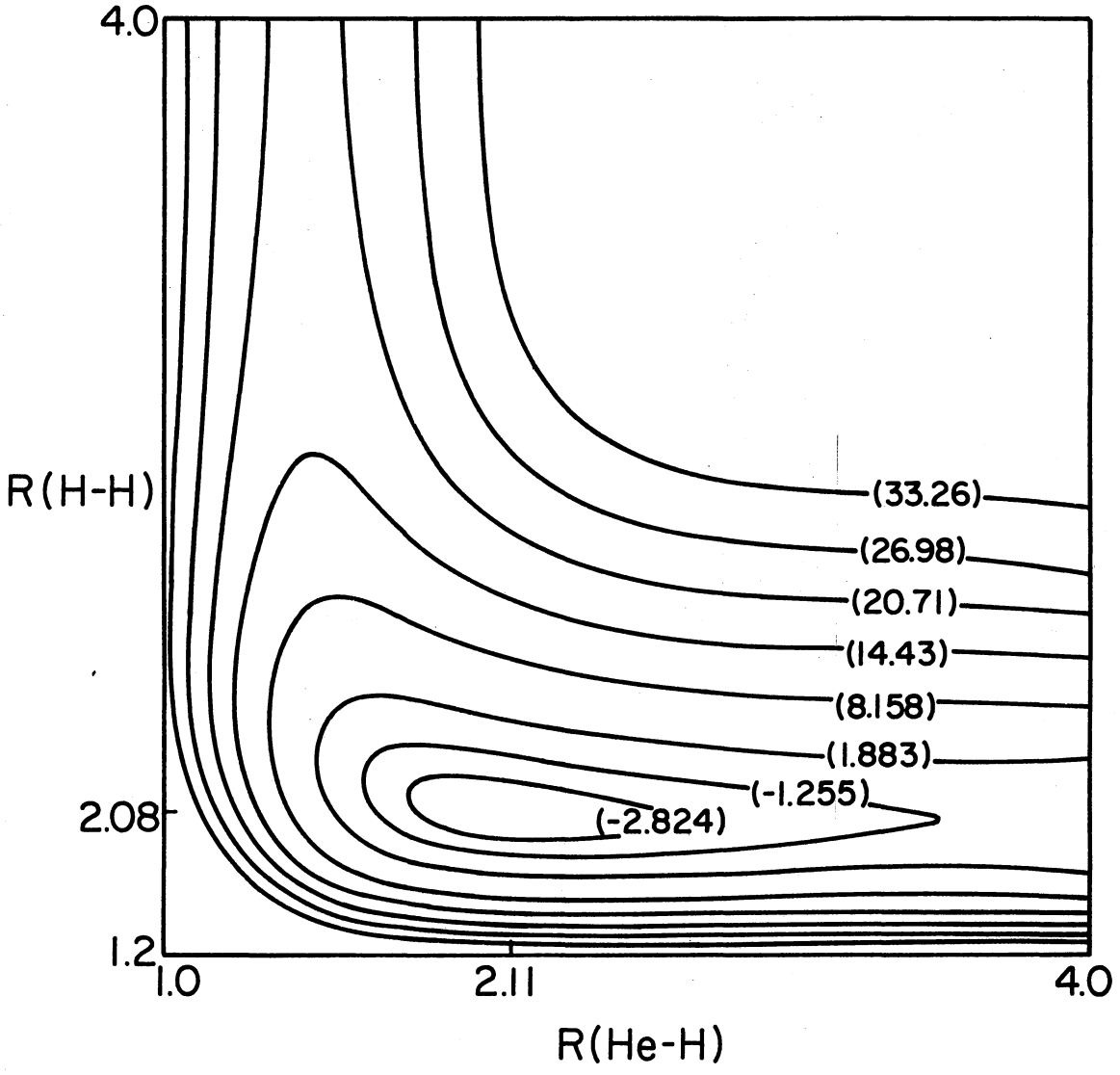

Figure 18. Contour Plot of the SAI Potential-Energy Surface for the Linear $HeHH^+$ System. Internuclear Separations are in Atomic Units. Energies are Given in Units of Kcal/mole Relative to the He + H_2^+ Asymptotic Limit

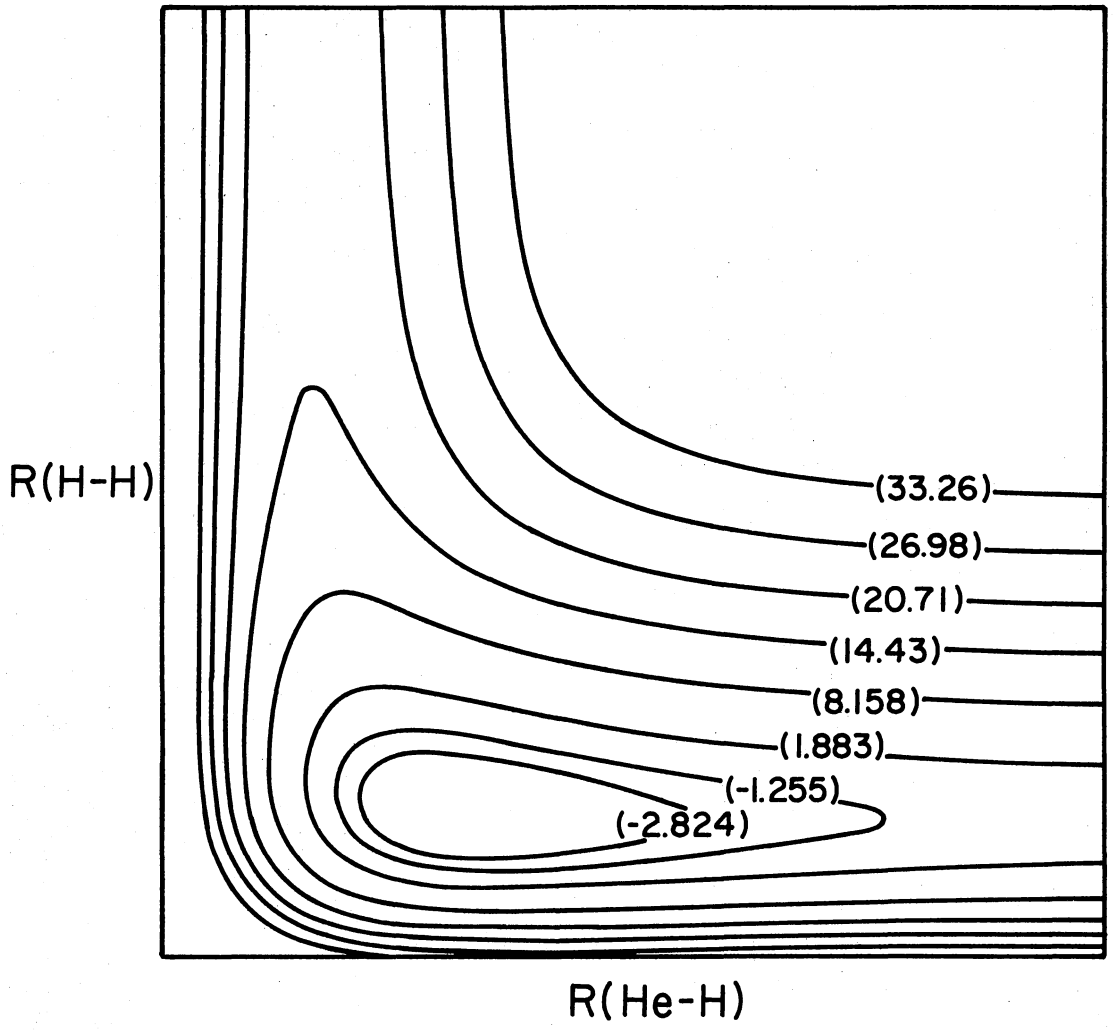

Figure 19. Contour Plot of the DIM Potential-Energy Surface for the Linear $HeHH^+$ System. Internuclear Separations are in Atomic Units. Energies are Given in Units of Kcal/mole Relative to the He + H_2^+ Asymptotic Limit

motion of the atoms was restricted to be collinear. The vibrational state was specified (v = 0-3) and the relative translational energy was chosen such that the sum of the vibrational energy and relative translational energy equals the total energy. The total energies were selected to be 0.94, 1.0, 1.1, 1.2 and 1.4 eV. Hamilton's equations were integrated numerically by Runge-Kutta-Gill procedure (1b) with a step size of 0.1 molecular units (1 time unit = $0.53871469 \times 10^{-14}$ sec. See reference (3)) except for the case of v = 0 and E_{trans} = 18.5 kcal/mole when a step size of 0.04 molecular units was used. 200 trajectories were computed for each set of initial vibrational and translational energies.

CHAPTER VI

RESULTS AND DISCUSSIONS

The results of QCT claculations on the collinear He + H_2^+ system using the DIM function for different initial vibrational states at various total energies have been described in Reference 21 and are reproduced in Figure 11. The calculations were repeated using a spline-fit of the DIM function (SDIM) on a (12 x 16) grid for total energy equal to 0.94 eV. The results are reported in Table X along with the DIM results. Figure 20 shows the results obtained by using the SAI surface.

Table X shows that SDIM results are in excellent agreement with the DIM results for the ground vibrational state of the hydrogen molecular ion. These results are in accord with previously reported studies on the (D + ClH) system (23a) that shows that splinefitted surfaces may be expected to yield the same average dynamical results as the analytic surface. The agreement between the results from the DIM surface and the SDIM surface is good for v = 1 and fair for the v = 2 state. Both calculations show the same trend as the earlier theoretical studies (19-21) on this system that vibrational energy does not enhance the total reaction probability. For v = 3 state however, the reaction probability obtained by using the SDIM surface is large whereas that by using the DIM is zero. This poor result occurs because, for the third vibrational state of the hydrogen molecular ion,

TABLE X

COMPARISON OF RESULTS USING THE DIM SURFACE AND THE SDIM SURFACE FOR TOTAL ENERGY EQUAL TO 0.94 eV

Vibrational State of H_2^+	Reaction Probability	
	DIM	SDIM
0	0.215	0.210
1	0.190	0.205
2	0.095	0.045
3	0.0	0.135

the inner classical turning point is less than 1.4 au, as illustrated in Figure 21, and it falls outside the region of the rectangular grid ($1.4 \leq R_1 \leq 8.0$, $1.4 \leq R_2 \leq 6.8$) used in the splinefit. Hence the derivatives used in the trajectory calculations are erroneous, leading to incorrect results. It is therefore clear that the splinefit reproduces the "original" potential-energy surface with reasonable accuracy and that as long as one stays within the region of (R_1-R_2) space spanned by the splinefit, no spurious effects are introduced.

Figure 20 shows that vibrational energy enhances the reaction probability for the He + H_2^+ reactive collisions except for the $v = 3$ state of the hydrogen molecular ion, for which the splinefit results may not be accurate. These results are qualitatively in accord with the experimental results given in Figure 16. In contrast, the previous QCT studies using the DIM function predicted the reverse trend that vibrational energy does not enhance the reaction probability

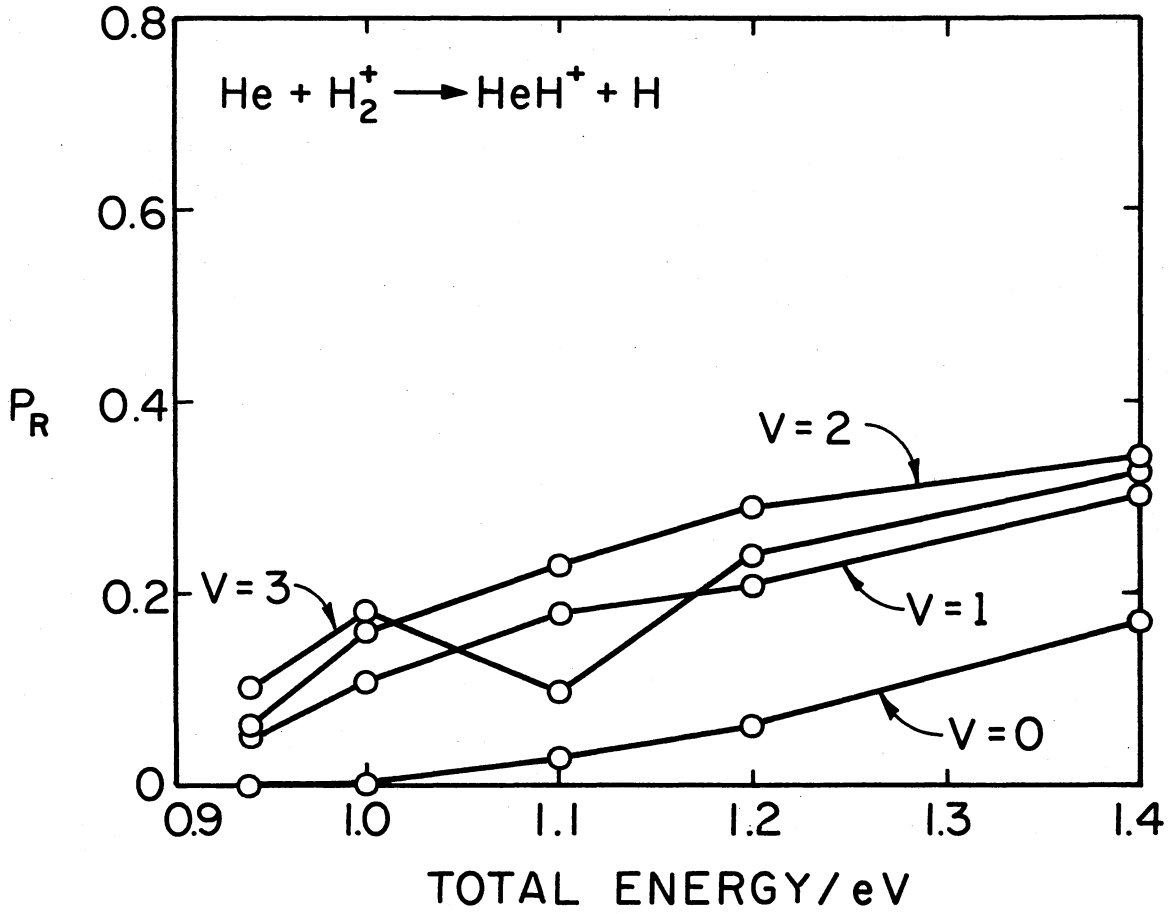

Figure 20. Quasiclassical Reaction Probability as a Function of Total Energy for Different Vibrational States Using Splinefitted Ab Initio Surface

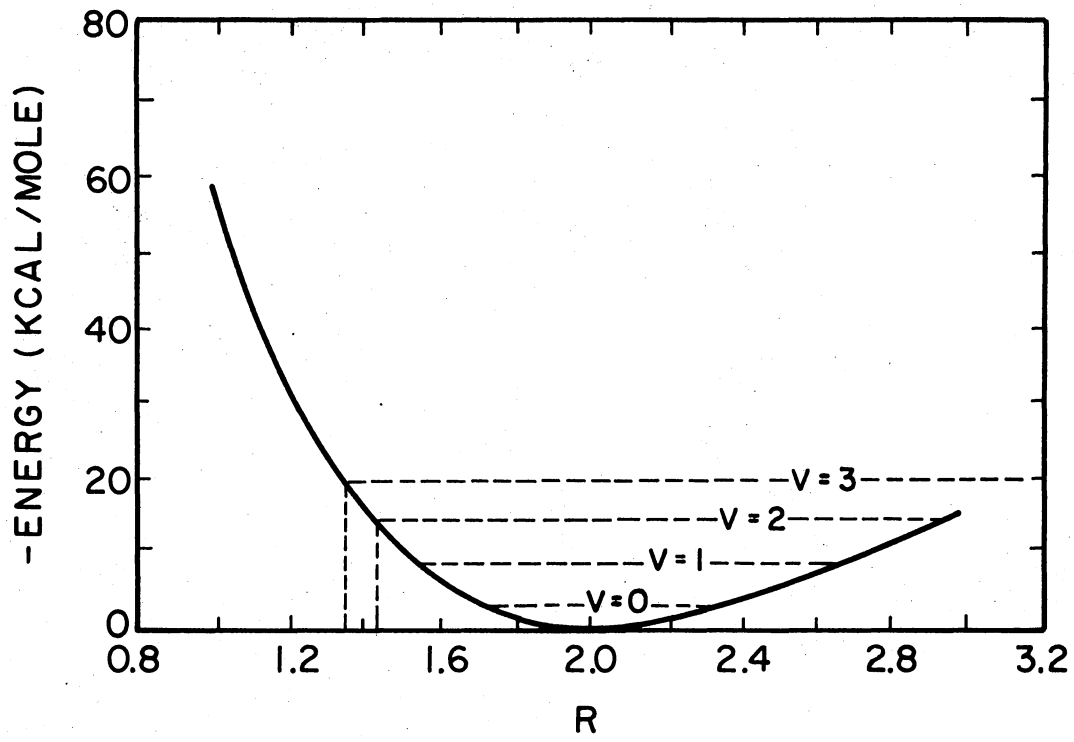

Figure 21. Vibrational States Plotted on the Morse Potential Energy Curve for H_2^+

for this system. The same result was also obtained by other two quantum mechanical calculations (19) (20) (26).

The only difference between the earlier studies and the present one is that they employed an analytic fit of the ab initio surface of Brown and Hayes (17) while the present study employed the two dimensional cubic splinefit of the same surface. Figures 18 and 19 illustrate that qualitatively the two surfaces are very similar, the main difference being that the analytic fit predicts a deeper well than the splinefit for the HeH_2^+ intermediate. Quantitatively, the splinefit deviates less from the ab initio values than the DIM function, as shown by the standard deviations for both surfaces in Table XI. The values for SAI surface in Table XI were obtained by removing one row of ab initio values from the grid and interpolating using 2D spline. From the earlier studies on different systems (13), this small difference between two potential-energy surfaces would be insufficient to explain the radically different dynamical results. However, Alexander and Berard (22) pointed out that small differences in potential-energy surfaces could lead to significantly different results. Furthermore, Duff and Truhlar (24) showed that two similar potential-energy surfaces for the H_2 + I system led to two very different results. They attributed this difference to the difference in the relative location of the region of maximum curvature of the reaction path. There the authors point out that vibrational excitation is expected to significantly enhance the reaction probability at a fixed total energy whenever the position of maximum reaction coordinate curvature comes before the increase in potential-energy along the reaction coordinate.

TABLE XI

COMPARISON OF THE ACCURACY OF THE
DIM AND SAI SURFACES

R(He-H)	R(H-H)	POTENTIAL-ENERGY		
		Ab initio	DIM	SAI
1.4	2.4	0.25321	0.21931	0.24775
1.6	2.4	-0.00677	-0.05289	-0.01007
1.8	2.4	-0.07202	-0.12233	-0.07433
2.0	2.4	-0.06335	-0.11027	-0.06562
2.4	2.4	0.00151	-0.02732	-0.00083
2.8	2.4	0.05559	0.04509	0.05145
3.6	2.4	0.11574	0.11915	0.11012
	Standard Deviation		0.01273	0.00014

Figure 22 gives the plot of potential-energy and curvature of the minimum energy path as a function of the reaction coordinate for the DIM and SAI surfaces. (The fine structures in the curvature for the SAI surface is not significant). In each case the reaction coordinate is almost identical. Furthermore, the variation in the curvature is also similar. However, the maximum for the DIM surface comes before the maximum for the SAI surface. Thus we would expect more vibrational enhancement for the former than for the latter. This, however, is not the case. It is therefore clear that subtle factors other than those discussed by Duff and Truhlar (24) are responsible for the computed differences.

It is gratifying to note that collinear QCT studies predict the qualitative features of the experimental results when an accurate ab initio potential-energy surface is used. A complete CI calculation of the potential-energy for this system (including the nonlinear conformations) is currently being carried out by McLaughlin and Thompson (25). Use of this surface will hopefully enable the quantitative prediction of the total reaction cross section for this system.

The present study does not seem to support the earlier suggestions (19) (21) (26) that the anomaly in the vibrational energy effect exhibited by the other theoretical results could be due to the collinear model employed. Such results are apparently due to the attempt to use an analytic DIM fit to the ab initio results. This system also seems to exhibit the "dynamic effect" (3) in that the reaction probability is zero for the reactant molecule in the ground vibrational state even though the total energy exceeds the reaction threshold. However, for the same total energy, higher

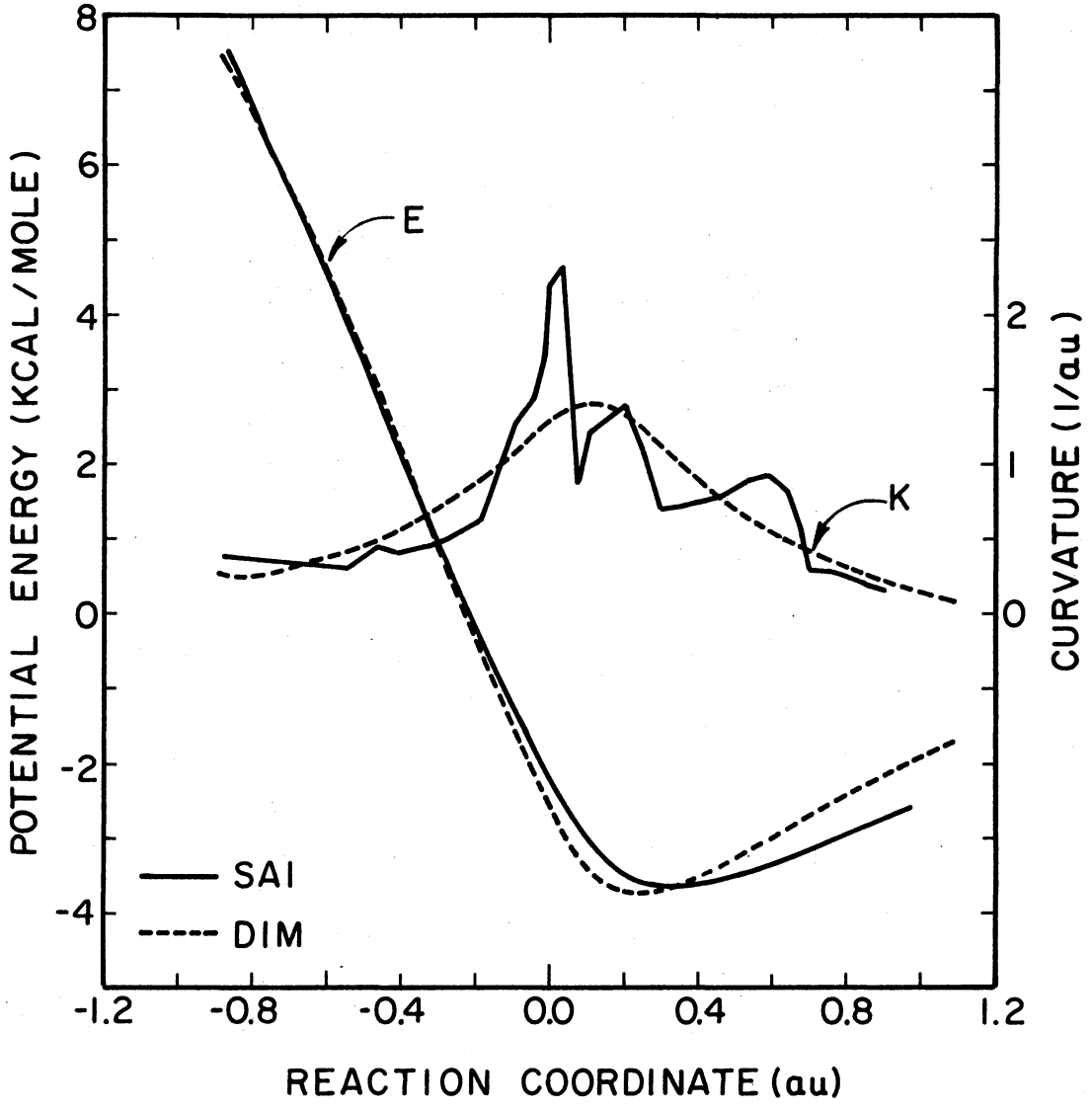

Figure 22. A Plot of the Curvature (1/au) of the Minimum Energy Path (Right Ordinate) and Potential-Energy in Kcal/mole (Left Ordinate) vs. the Reaction Coordinate (au) Measured from the Equal Displacement Distance for the Exothermic Reaction $HeH^+ + H \rightarrow He + H_2^+$

vibrational states of the reactant molecule are efficient in producing reactive collisions.

Conclusion

The present study clearly shows that the cubic spline interpolation method is a versatile tool in interpolating ab initio potential-energy surfaces and that the quasiclassical trajectory studies are able to predict the correct experimental results, if only qualitatively.

BIBLIOGRAPHY

(1) (a) M. Karplus, R. N. Porter and R. D. Sharma, J. Chem. Phys. 43, 3259 (1963).

(b) R. N. Porter and L. M. Raff in "Modern Theoretical Chemistry", Chap. VIII in Vol. 3, "Dynamics of Molecular Collisions", (Ed: W. H. Miller), (Plenum, New York, 1975).

(2) L. M. Raff, H. H. Suzukawa, Jr. and D. L. Thompson, J. Chem. Phys. 62, 3743 (1975).

(3) L. M. Raff, D. L. Thompson, L. B. Sims and R. N. Porter, J. Chem. Phys. 56, 5998 (1972).

(4) J. C. Polanyi, Acconts. Chem. Research 5, 161 (1972).

(5) L. M. Raff, J. Chem. Phys. 60, 2220 (1974).

(6) (a) J. C. Polanyi and J. L. Schreiber, in "Physical Chemistry-An Advanced Treatise", (Ed: H. Eyring, W. Jost and D. Henderson) Vol. 6a, "Kinetics of Gas Reactions", Chap. 6, (Academic Press, New York), 1974) p. 383.

(b) R. N. Porter, Ann. Rev. Phys. Chem. 25, 317 (1974).

(7) K. R. Symon, "Mechanics", (Addison-Wesley Publishing Co., 1971), p. 392.

(8) W. S. Dorn and D. D. McCracken, "Numerical Methods with Fortran Case Studies", (John Wiley & Sons, Inc., 1972), pp. 267-284.

(9) (a) J. B. Anderson, J. Chem. Phys. 52, 3849 (1970).

(b) K. G. Anlauf, P. J. Kuntz, D. H. Maylotte, P. D. Pacey and J. C. Polanyi, Disc. Faraday. Soc. 44, 183 (1967); J. C. Polanyi and S. D. Rosner, J. Chem. Phys. 38, 1028 (1963).

(c) F. T. Wall and R. N. Porter, J. Chem. Phys. 39, 3112 (1963); F. T. Wall, L. A. Hiller, Jr. and J. Mazur, J. Chem. Phys. 35, 1284 (1961).

(d) C. A. Parr, J. C. Polanyi and W. H. Wong, J. Chem. Phys. 58, 5 (1973).

(e) P. J. Kuntz, E. M. Nameth, J. C. Polanyi, S. D. Rosner and C. E. Young, J. Chem. Phys. 44, 1168 (1966).

(f) D. L. Bunker and N. C. Blais, J. Chem. Phys. 41, 2377 (1964).

(g) D. L. Bunker and C. A. Parr, J. Chem. Phys. 52, 5700 (1970).

(h) D. L. Bunker and M. D. Pattengill, J. Chem. Phys. 53, 3041 (1970).

(i) R. L. Jaffe and J. B. Anderson, J. Chem. Phys. 54, 2224 (1971); R. L. Jaffe, J. M. Henry and J. B. Anderson, J. Chem. Phys. 59, 1128 (1972).

(j) P. J. Kuntz, E. M. Nameth and J. C. Polanyi, J. Chem. Phys. 50, 4607 (1969).

(k) P. J. Kuntz, M. H. Mok and J. C. Polanyi, J. Chem. Phys. 50, 4623 (1969).

(l) P. J. Kuntz, E. M. Nameth, J. C. Polanyi and W. H. Wong, J. Chem. Phys. 52, 4654 (1970).

(m) J. T. Muckerman, J. Chem. Phys. 54, 1155 (1971).

(n) M. H. Mok and J. C. Polanyi, J. Chem. Phys. 53, 4588 (1970).

(o) J. C. Polanyi and W. H. Wong, J. Chem. Phys. 51, 1439 (1969).

(p) R. L. Wilkins, J. Chem. Phys. 57, 912 (1972).

(q) D. L. Thompson, J. Chem. Phys. 56, 3570 (1972).

(r) L. M. Raff, D. L. Thompson, L. B. Sims and R. N. Porter, J. Chem. Phys. 56, 5998 (1972).

(s) R. N. Porter, D. L. Thompson, L. M. Raff and J. M. White, J. Chem. Phys. 62, 2429 (1975).

(t) J. B. Anderson and R. T. V. Kung, J. Chem. Phys. 58, 2477 (1972).

(u) L. M. Raff, J. Chem. Phys. 46, 520 (1967).

(v) S. Chapman and J. Suplinskas, J. Chem. Phys. 60, 248 (1974).

(w) L. M. Raff, J. Chem. Phys. 44, 1202 (1962); L. M. Raff and M. Karplus, J. Chem. Phys. 44, 1212 (1966).

(10) N. Sathyamurthy and L. M. Raff, J. Chem. Phys. 63, 464 (1975).

(11) L. M. Raff, L. Stivers, R. N. Porter, D. L. Thompson and L. B. Sims, J. Chem. Phys. 52, 3449 (1970).

(12) Chem. Eng. News, 53,(18), 4(1975).

(13) (a) A + BC: D. S. Berry, J. C. Polanyi and C. W. Wilson, Jr., Chem. Phys. 3, 317 (1974).

(b) H + HBr: J. M. White and D. L. Thompson, J. Chem. Phys. 61, 719 (1974).

(c) Br + HCl: D. J. Douglas, J. C. Polanyi and J. J. Sloan, J. Chem. Phys. 59, 6679 (1973).

(d) H_2 + I: R. N. Porter, L. B. Sims, D. L. Thompson and L. M. Raff, J. Chem. Phys. 58, 2855 (1973).

(e) H_2 + I_2: Reference 3.

(f) H + HF: Reference 9a.

(g) A + BC: G. E. Kellerhals, Ph.D. Thesis, Oklahoma State University, Stillwater, Oklahoma.

(h) F + H_2: G. C. Schatz, J. M. Bowman and A. Kupperman, J. Chem. Phys. 58, 4023 (1973).

(14) (a) K. G. Anlauf, D. M. Maylotte, J. C. Polanyi and R. B. Bernstein, J. Chem. Phys. 51, 5716 (1969).

(b) J. C. Polanyi and D. C. Tardy, J. Chem. Phys. 51, 5717 (1969).

(c) K. G. Anlauf, P. J. Kuntz, D. H. Maylotte, P. D. Pacey and J. C. Polanyi, Discuss. Faraday. Soc. 44, 183 (1967).

(d) K. G. Anlauf, P. E. Charters, D. S. Horne, R. G. Macdonald, D. H. Maylotte, J. C. Polanyi, W. J. Skrlac, D. C. Tardy and K. B. Woodall, J. Chem. Phys. 53, 4091 (1970).

(15) J. Dubrin and M. J. Henchman in MTP International Review of Science, Physical Chemistry Series One. vol. 9, "Chemical Kinetics", (Ed: J. C. Polanyi, University Park Press, Baltimore, 1972), p. 213.

(16) (a) W. A. Chupka, J. Berkowitz and M. E. Russell, "VII International Conference on the Physics of Electronic and Atomic Collisions", (M.I.T., Cambridge, Mass. 1969), p. 71.

(b) W. A. Chupka, M. E. Russell and K. Refaey, J. Chem. Phys. 48, 1518 (1968).

(c) L. P. Theard and W. T. Huntress, Jr., J. Chem. Phys. 60, 2840 (1974).

(d) R. Johnsen and M. A. Biordi, J. Chem. Phys. 61, 2112 (1974).

(17) P. J. Brown and E. F. Hayes, J. Chem. Phys. 55, 922 (1971).

(18) P. J. Kuntz, Chem. Phys. Lett. 16, 581 (1972).

(19) D. J. Kouri and M. Baer, Chem. Phys. Lett. 24, 37 (1974).

(20) J. T. Adams, "Collinear Quantum Mechanical Calculations for the Reaction: $He + H_2^+ \rightarrow HeH^+ + H$ (to be published).

(21) N. Sathyamurthy, Ph.D. Thesis, Oklahoma State University, Stillwater, Oklahoma (1975).

(22) M. H. Alexander and E. V. Berardm J. Chem. Phys. 60, 3950 (1974).

(23) (a) Reference 10.

(b) D. R. Mclaughlin and D. L. Thompson, J. Chem. Phys. 59, 4393 (1973).

(24) J. W. Duff and D. G. Truhlar, J. Chem. Phys. 62, 2477 (1975).

(25) D. R. Mclaughlin and D. L. Thompson (private communication).

(26) P. J. Kuntz and W. N. Whitton, Chem. Phys. Lett. 34, 340 (1975).

VITA

Radha Rangarajan

Candidate for the Degree of

Master of Science

Thesis: I. STUDY OF THE EFFECT OF INTEGRATION STEP SIZE IN QUASICLASSICAL TRAJECTORY CALCULATIONS

II. STUDY OF THE ROLE OF VIBRATIONAL ENERGY IN REACTIVE COLLISIONS: $He + H_2^+ \rightarrow HeH^+ + H$ USING SPLINEFITTED AB INITIO AND DIM POTENTIAL-ENERGY SURFACES

Major Field: Chemistry

Biographical:

Personal Data: Born in India, December 7, 1953.

Education: Graduated from Government Girls' High School, Chidambaram, India in April, 1970; received the Bachelor of Science degree from Annamalai University, India in May, 1974; completed requirements for the Master of Science degree at Oklahoma State University, December, 1975.

Professional Experience: Government of India Merit Scholar, 1970; Graduate Excellence Awardee, Oklahoma State University, Spring 1975; Special Summer Scholarship Awardee, Oklahoma State University, Summer 1975; Graduate Teaching Assistant, Oklahoma State University, 1974-1975.

Membership in Honorary and Professional Societies: Member of Phi Lambda Upsilon, Honorary Chemical Society.